AD_____

Award Number:
W81XWH-13-1-0199

TITLE: Targeting Master Regulators of the Breast Cancer Metastasis Transcriptome

PRINCIPAL INVESTIGATOR: Timothy A. Chan MD, PhD

CONTRACTING ORGANIZATION: Sloan-Kettering Institute for Cancer Research
NEW YORK NY 10065-6007

REPORT DATE: July 2014

TYPE OF REPORT: annual

PREPARED FOR: U.S. Army Medical Research and Materiel Command
Fort Detrick, Maryland 21702-5012

DISTRIBUTION STATEMENT: Approved for Public Release;
Distribution Unlimited

The views, opinions and/or findings contained in this report are those of the author(s) and should not be construed as an official Department of the Army position, policy or decision unless so designated by other documentation.

REPORT DOCUMENTATION PAGE

Form Approved
OMB No. 0704-0188

1. REPORT DATE	2. REPORT TYPE	3. DATES COVERED
July 2014	annual	1 July 2013 - 30 June 2014

4. TITLE AND SUBTITLE
Targeting Master Regulators of the Breast Cancer Metastasis Transcriptome

5a. CONTRACT NUMBER

5b. GRANT NUMBER
W81XWH-13-1-0199

5c. PROGRAM ELEMENT NUMBER

6. AUTHOR(S)
Timothy A. Chan

E-Mail: chant@mskcc.org

5d. PROJECT NUMBER

5e. TASK NUMBER

5f. WORK UNIT NUMBER

7. PERFORMING ORGANIZATION NAME(S) AND ADDRESS(ES)
AND ADDRESS(ES)
SLOAN-KETTERING INSTITUTE FOR CANCER RESEARCH
NEW YORK NY 10065-6007

8. PERFORMING ORGANIZATION REPORT NUMBER

9. SPONSORING / MONITORING AGENCY NAME(S) AND ADDRESS(ES)
U.S. Army Medical Research and Materiel Command
Fort Detrick, Maryland 21702-5012

10. SPONSOR/MONITOR'S ACRONYM(S)

11. SPONSOR/MONITOR'S REPORT NUMBER(S)

12. DISTRIBUTION / AVAILABILITY STATEMENT
Approved for Public Release; Distribution Unlimited

13. SUPPLEMENTARY NOTES

14. ABSTRACT

The goal of our work is to characterize and target the master regulators of the breast cancer metastasis transcriptome. We seek to elucidate the key factors controlling large scale genetic programs that bring about the metastasis phenotype and to discover ways to target these regulators. To this end, this year, we have made substantial progress. We have comprehensively completed transcriptome profiling of the largest set of breast cancer primary/metastasis matched pairs that we know of. We have characterized the gene expression programs and the corresponding master regulators of these programs. The first major program we have worked out is that of neoangiogenesis. We showed that our top regulators control metastasis vasculogenesis by controlling RECK, which in turn, orchestrates a highly coordinated neoangiogenic switch. We have also developed in vitro and genomic platforms that will enable us to work out the blueprint of the hierarchy of regulators controlling the metastasis gene program.

15. SUBJECT TERMS
metastasis, transcriptome, breast cancer, angiogenesis

16. SECURITY CLASSIFICATION OF:			17. LIMITATION OF ABSTRACT	18. NUMBER OF PAGES	19a. NAME OF RESPONSIBLE PERSON
a. REPORT	b. ABSTRACT	c. THIS PAGE			USAMRMC
U	U	U	UU	25	19b. TELEPHONE NUMBER *(include area code)*

Table of Contents

Page

Era of Hope Annual Progress Report, July 2014

PI: Timothy A. Chan

Introduction

The vast majority of breast cancer deaths are due to metastatic progression. The central tenet underlying our work is that master regulators of the metastasis transcriptome are fundamentally important for the metastatic process and that systematic understanding of these changes will be of tremendous clinical diagnostic value and help lay the foundation for effective treatments to eradicate breast cancer. Understanding the ultimate drivers of metastasis is a crucial step in achieving the goal of a cure for metastatic disease. Through a systematic approach employing global, large-scale analysis of primary tumors and metastases, rigorous state-of-the-art bioinformatic analysis, and functional models using isogenic human breast cancer cells with varying metastatic potential, we will work to elucidate the mechanisms underlying our candidates as master regulators of breast cancer metastasis. We are developing methods to target these candidates using small molecules. Our specific research goals are the following. (Aim 1) First, we will elucidate the effects of our top candidates on the breast cancer metastasis transcriptome and epigenome. These studies will utilize microarray and next-generation sequencing technologies. We will define how these candidates remodel the transcriptome and epigenome to promote metastasis. (Aim 2) Second, we will determine the dependence of breast cancer metastasis on our candidates in both hormone positive and negative breast cancers. We will study the physiologic basis of how these genes regulate the metastatic process using both in vitro models and multiple mouse models of metastasis. And, we will apply our results to the clinic by determining the prognostic value of varying levels of our candidates in primary tumors. (Aim 3) Third, we will develop an approach to target our candidates to inhibit breast cancer metastasis using small molecules.

Keywords

metastasis, regulator, breast cancer, transcriptome, epigenetic

Overall Project Summary

For the first funding year, we have concentrated on Tasks 1 and 2 in the Statement of Work. This was to (1) elucidate the effects of our candidate master regulators of metastasis on the breast cancer metastasis transcriptome and (2) to determine the dependence of breast cancer metastasis on master regulators such as Trim25 and BRD8). To the end, we have made significant progress and are on track.

A primary effort this year was to evaluate the effects of expression of master regulators BRD8 and TRIM25 using global approaches. We have performed many of these analyses. Using both overexpression and knockout systems, examined the individual effector pathways which are regulated by these proteins. We have also completed our analysis of primary breast tumors and matched metastases using expression arrays and compared these results to the in vitro expression models. We compared these results to that of the in vitro cellular systems using GSEA and transcriptional module mapping.

Our data shows that one of the top GSEA enriched pathways regulated by TRIM25 and BRD8 is the neoangiogenesis pathway. These two genes converge to regulate a protein called RECK. We showed that RECK is shut off selectively in metastases and this change in expression also is associated with markedly increased likelihood of metastasis.

We went further and dissected the mechanism by which this happened. We showed that during development of metastasis, RECK controls a Stat3-dependent neoangiogenic switch. Its does this by associating with gp130 and multiple Stat3-dependent receptors on the cell membrane. Therefore, BRD8/TRIM25 is able to control angiogenesis by downregulating RECK, which controls a large angiogenic program. We showed that the effectors of this program includes multiple terminal effectors of angiogenesis, such as uPAR, VEGF, and others. Interestingly, this program is highly dependent in vivo on Stat3, as Stat3 can rescue a RECK loss phenotype. These results were published in *Oncogene* in 2014. This report puts RECK and the RECK-controlled angiogenic switch firmly within the regulomes governed by the metastasis master regulator candidates. It also answers the long sought question of what the root drivers of the neoangiogenic cascade in metastases are.

We are also actively working to develop systems to analyze the genome-wide targets of TRIM25 and BRD8 using CHIP-seq. So far, we have optimized antibodies for CHIP. Using CHIP followed by DNA bioanalysis, we have confirmed that TRIM25 and BRD8 associate with chromatin. These results are required as a required step to our eventual goal of characterizing how TRIM25 and BRD8 modulates the epigenome.

Lastly, this year, we have also made progress in our work on generating a blueprint of the master regulator hierarchy governing metastasis. As noted in our preliminary data, we have identified a collection of master regulators that control the metastasis transcriptome. TRIM25 and BRD8 are among the top ranking transcription factors among a set of 20 which control various arms of the metastasis program. We have now knocked down all 20 in pairwise combinations so that we can detect cooperativity. These will be analyzed using RNAseq this coming year. This critical experiment will be one of the foundations of Task 1 and it is progressing nicely.

In summary, we have made good progress. We are looking forward to continuing this work with the DOD.

Key Research Accomplishments

- Established overexpression and knockdown systems for TRIM25, BRD8 and multiple other top candidate master regulators required for the study of genomic changes leading to metastasis. These systems are a significant resource for the metastasis field.
- Characterization of the neoangiogenic genetic program of BRD8 and TRIM25 as being directed by silencing of RECK in metastatic lesions
- RECK coordinately controls a orchestrated neoangiogenic switch during development of breast cancer metastases and is responsible for the angiogenic phenotype in metastases

Conclusions

In summary, we have made substantial progress toward our aims during year 1. The aims have not changed. This year, we have completed metastasis transcriptome profiling and characterization. We have characterized a major arm of this program – the neoangiogenic arm – controlled by the metastasis regulators as involving the metastasis suppressor RECK. We have comprehensively worked out how RECK causes the vascularization that is required for metastases to take root. We have also established innovative reagents to study the master regulators, which will benefit the field as a whole. Plans for this coming year are to proceed with the aims as outlined in the grant. We plan to use transcriptome profiling of TRIM25/BRD8 and other master regulators to work out the regulatory hierarchy. We also plan to begin the work with mice to model the effects of the master regulators on breast cancer metastasis.

Publications/References

Walsh LA, Roy DM, Reyngold M, Giri D, Snyder A, Turcan S, Badwe CR, Lyman JL, Bromberg J, King TA, and **Chan TA***. RECK controls breast cancer metastasis by modulating a convergent, STAT3-dependent neoangiogenic switch. ***Oncogene*** 2014. June 16. PMID: 24931164.

Inventions, Patents, and Licenses

Nothing to report

Reportable Outcomes

Nothing to report

Other Achievements

Nothing to report

BIOGRAPHICAL SKETCH

Provide the following information for the Senior/key personnel and other significant contributors.
Follow this format for each person. **DO NOT EXCEED FOUR PAGES.**

NAME	POSITION TITLE
Timothy A. Chan	Associate Member/ Associate Professor Human Oncology and Pathogenesis Program Memorial Sloan-Kettering Cancer Center
eRA COMMONS USER NAME (credential, e.g., agency login) CHANTMSKCC	

EDUCATION/TRAINING *(Begin with baccalaureate or other initial professional education, such as nursing, include postdoctoral training and residency training if applicable.)*

INSTITUTION AND LOCATION	DEGREE *(if applicable)*	MM/YY	FIELD OF STUDY
Harvard University, Cambridge, MA	AB	1991-1995	Biochemical Sciences (*Summa cum laude*)
Johns Hopkins School of Medicine, Baltimore, MD	PhD	1997-2002	Human Genetics and Biochemistry
Johns Hopkins School of Medicine, Baltimore, MD	MD	1995-2002	Medicine (M.D./Ph.D. program)
Mercy Hospital/Univ. of Maryland, Baltimore, MD	Internship	2002-2003	Internal Medicine
Johns Hopkins Hospital, Baltimore, MD	Residency	2003-2007	Radiation Oncology
Chief Resident, Johns Hopkins Hospital, Baltimore, MD		2006-2007	Radiation Oncology
Johns Hopkins School of Medicine, Baltimore, MD	Fellowship	2006-2007	Cancer Biology

A. Personal Statement

Timothy A. Chan MD, PhD, is an Associate Member and Attending Physician at the Memorial Sloan-Kettering Cancer Center (MSKCC), Vice Chair of the Dept. of Radiation Oncology, and Associate Professor at the Weill Cornell School of Medicine. He is PI of a cancer genetics laboratory and is an expert in the study of tumor suppressor genes. Dr. Chan received an MD, a PhD in cancer genetics, completed a residency in Radiation Oncology, and a fellowship in cancer genomics and epigenomics. The Chan laboratory specializes in using genomic analysis to characterize the role of tumor suppressors in oncogenesis and in using multiple approaches for the study of cancer genes. These approaches include large-scale analyses, functional genomics, epigenomics, biochemical and molecular analyses, and mouse modeling. The lab has a special interest in deciphering the mechanisms underlying treatment response. He is also an integral part of the clinical teams at MSKCC and thus is in a unique position to effectively integrate his studies in the laboratory and efforts involving clinical treatments and samples. Dr. Chan is part of a multidisciplinary, collaborative research team that has the scope and breadth of expertise needed to obtain definitive outcomes for the studies proposed, and is dedicated to the success of this project.

B. Positions and Honors

Positions and Employment

1989-1991	Structure and function of *src* family proto-oncogenes during development. Advisor: Prof. Robert E. Steele. Dept. of Biochemistry and Molecular Biology, UC Irvine, CA. Research assistant.
1992, summer	Gene targeting using recombinant adenoviruses. Advisor: Prof. Milton Taylor. Dept. of Biology, Indiana University, Bloomington , IN. Research assistant.
1991-1992	Biochemical and functional analysis of the human liver extracellular ATPase. Advisor: Prof. Guido Guidotti. Dept. of Biochemistry, Harvard University, Cambridge, MA. Research assistant.
1993, summer	Cell cycle regulation of histone gene expression. Post-transcriptional regulation of tumor

	necrosis factor. Advisor: Prof. William F. Marzluff. Program in Molecular Biology and Biotechnology, Univ. of North Carolina, Chapel Hill, NC. Undergraduate research fellow.
1993-1995	Molecular mechanisms of axon guidance. Investigated the function of N-CAM and L1 in axon guidance using chromophore-assisted laser inactivation. Advisor: Prof. Daniel G. Jay. Dept. of Molecular and Cellular Biology, Harvard University, Cambridge, MA. Undergraduate thesis.
1994, summer	Function of the cyclin-dependent kinase inhibitors p21 and p15. Identification and characterization of mutations in the p15 tumor suppressor in human cancers. Advisors: Dr. David Beach, Dr.Gregory J. Hannon. Cold Spring Harbor Laboratory, Cold Spring Harbor, NY. Undergraduate research fellow.
1996-2002	Ph.D. thesis research on G2 checkpoint control following DNA damage. Described mechanisms of the p53-dependent G2 checkpoint. Identified and characterized 14-3-3 sigma as a key effector of p53- induced G2 cell cycle arrest. Developed new and efficient methods to engineer targeted genetic alterations in human cells. Advisor: Prof. Bert Vogelstein. Dept. of Oncology, Johns Hopkins School of Medicine, Baltimore, MD. PhD thesis.
7/06-6/07	Post-doctoral fellow, Epigenetic mechanisms of carcinogenesis. Advisor: Prof. Steve Baylin. Dept. of Oncology, Johns Hopkins School of Medicine, Baltimore, MD
8/2007-present	Assistant Member, Dept. of Radiation Oncology and Human Oncology and Pathogenesis Program, Memorial Sloan-Kettering Cancer Center, New York, NY
8/2008-present	Assistant Professor, Gerstner Sloan-Kettering Graduate School of Biomedical Sciences, Memorial Sloan-Kettering Cancer Center, NY
5/2009-present	Beene Translational Oncology Core, Faculty advisor, Memorial Sloan-Kettering Cancer Center
5/2010-present	The Cancer Genome Atlas, Colorectal Disease, MSKCC, Principal Investigator
9/2009-present	Co-director, MSKCC Acoustic Neuroma Service
2010-present	TCGA Colorectal Leadership, Analysis Working Group and Writing Committee
2010-present	Assistant Professor, Weill Cornell School of Medicine
2012-present	Associate Member, Human Oncology and Pathogenesis Program and Dept of Radiation Oncology, Memorial Sloan-Kettering Cancer Center, New York, NY
2012-present	Associate Professor, Gerstner Sloan-Kettering Graduate School of Biomedical Sciences, Memorial Sloan-Kettering Cancer Center, NY
2013-present	Vice Chair, Dept. of Radiation Oncology
2013-present	Director of Translational Oncology, Dept. of Radiation Oncology

Other Experience and Professional Memberships

2007-present	American Association for Cancer Research (AACR)
2003-present	American Society for Therapeutic Radiology and Oncology (ASTRO)
2006-present	American Society of Clinical Oncology (ASCO)
1998-present	Admissions Advisor, Harvard College Admissions Committee.
2007-present	Scientific Review Committee, American Society for Therapeutic Radiology and Oncology
5/2010-present	The Cancer Genome Atlas Project Analysis Working Group, member
2010-present	Scientific Advisory Board, Cancer Genetics, Inc. (New York)
2011-present	Scientific Advisory Board, QuanDx, Inc.

Honors

1994	Barry Goldwater National Science Prize
1994	Cold Spring Harbor Laboratory Undergraduate Research Program
1995	Phi Beta Kappa (top 24 of class of 1995 at Harvard College)
1995-2002	NIH Medical Scientist Training Program
1996	Howard Hughes Medical Institute Research Fellowship
2001	Paul Erlich Prize: awarded for excellence in research
2002	Johns Hopkins Fellows Research Award: for outstanding research
2005	ASTRO Young Investigator Travel Award
2005	ASTRO Translational Research Travel Award
2005	ASTRO Award of Merit: for outstanding research
2006	Young Investigator Award, American Society of Clinical Oncology
2008	FAMRI Clinical Scholar
2008	Louis Gerstner Investigator Award

2009 Doris Duke Clinical Scientist Award
2010 Sontag Distinguished Scientist Award
2012 DOD Era of Hope Scholar
2013 Frederick Adler Chair

C. Selected Peer-reviewed Publications (15 selected out of 77, in chronological order)

1. **Timothy A. Chan**, Patrice J. Morin, Bert Vogelstein, and Kenneth W. Kinzler (1998) Mechanisms underlying nonsteroidal anti-inflammatory drug-induced apoptosis. **Proceedings of the National Academy of Sciences USA** 95, 681-686. PMCID: PMC18480.
2. **Timothy A. Chan**, Heiko Hermeking, Christoph Lengauer, Kenneth W. Kinzler, and Bert Vogelstein (1999) 14-3-3σ is required to prevent mitotic catastrophe following DNA damage. **Nature** 401, 616-620. (featured article in News & Views) PMID: 10524633.
3. Tong-chuan He, **Timothy A. Chan**, Bert Vogelstein, and Kenneth W. Kinzler (1999) PPARδ is an APC regulated target of nonsteroidal anti-inflammatory drugs. **Cell** 99, 335-345. NIHMSID: 513730.
4. **Timothy A. Chan**, Paul M. Hwang, Heiko Hermeking, Kenneth W. Kinzler, and Bert Vogelstein (2000) Cooperative effects of genes controlling the G2/M checkpoint. **Genes and Development** 14, 1584-1588. PMCID: PMC316737.
5. **Timothy A. Chan**, Zhenghe Wang, Long H. Dang, Bert Vogelstein, and Kenneth W. Kinzler (2002) Targeted inactivation of CTNNB1 reveals unexpected effects of beta-catenin mutation. **Proceedings of the National Academy of Sciences USA** 99, 8265-8270. PMCID: PMC123056.
6. **Timothy A. Chan**, Sabine Glockner, Joo Mi Yi, Wei Chen, Leander van Neste, Leslie Cope, James G. Herman, Victor Velculescu, Kornel E. Schuebel, Nita Ahuja, Stephen B. Baylin (2008) Convergence of mutation and epigenetic alterations identifies common genes in cancer that predict for poor prognosis. **PLoS Medicine** 5 (5) 823-837. PMCID: PMC2429944.
7. Selvaraju Veeriah, Cameron Brennan, Shasha Meng, Fang Fang, Bhuvanesh Singh, James A. Fagin, David B. Solit, Philip B. Paty, Dan Rohle, Igor Vivanco, Juliann Chmielecki, William Pao, Marc Ladanyi, William L.Gerald, Linda Liau, Timothy C. Cloughesy, Paul S. Mischel, Chris Sander, Barry Taylor, Nikolaus Schultz, John Major, Adriana Heguy, Ingo K. Mellinghoff, and **Timothy A. Chan** (2009) The protein tyrosine phosphatase PTPRD is a tumor suppressor that is frequently inactivated and mutated in glioblastoma and other human cancers. **Proceedings of the National Academy of Sciences USA** 106, 9435-9440. PMCID: PMC2687998.
8. Selvaraju Veeriah, Barry S. Taylor, Shasha Meng, Fang Fang, Emrullah Yilmaz, Igor Vivanco, Manickam Janakiraman, Nikolaus Schultz, Aphrothiti J. Hanrahan, William Pao, Marc Ladanyi, Chris Sander, Adriana Heguy, Eric C. Holland, Phillip B. Paty, Paul S. Mischel, Linda Liau, Timothy F. Cloughesy, Ingo K. Mellinghoff, David B. Solit, **Timothy A. Chan** (2010) Somatic mutations of the Parkinson's Disease gene PARK2 in glioblastoma and other human malignancies. **Nature Genetics** 42, 77-82. PMID: 19946270.
9. Fang Fang, Sevin Turcan, Andreas Rimner, Andrew Kaufman, Dilip Giri, Luc G. T. Morris, Ronglai Shen, Venkatraman Seshan, Qianxing Mo, Adriana Heguy, Stephen B. Baylin, Nita Ahuja, Agnes Viale, Joan Massague, Larry Norton, Linda T. Vahdat, Mary Ellen Moynahan, and **Timothy A. Chan** (2011) Breast Cancer Methylomes Establish an Epigenomic Foundation for Metastasis. **Science Translational Medicine** 3, 1-12. (featured article) PMCID: PMC3146366.
10. Luc G.T. Morris, Barry S. Taylor, Trever G. Bivona, Yongxing Gong, Stephanie Eng, Cameron Brennan, Andrew Kaufman, Edward R. Kastenhuber, Victoria E. Banuchi, Bhuvanesh Singh, Adriana Heguy, Agnes Viale, Ingo K. Mellinghoff, Jason Huse, Ian Ganly, and **Timothy A. Chan** (2011) Genomic dissection of the EGFR/PI3K pathway reveals frequent deletion of the EGFR phosphatase PTPRS in head and neck cancers. **Proceedings of the National Academy of Sciences USA** 108, 19024-9. PMCID: PMC3223475.
11. Chao Lu, Patrick S. Ward, Gurpreet S. Kapoor, Dan Rohle, Sevin Turcan, Omar Abdel-Wahab, Christopher Edwards, Raya Khanin, Maria E. Figueroa, Ari Melnick, Kathryn E. Wellen, Donald M. O'Rourke, Shelley L. Berger, **Timothy A. Chan**, Ross L. Levine, Ingo K. Mellinghoff and Craig B. Thompson. (2012) IDH mutation impairs histone demethylation and results in a block to cell differentiation. **Nature** (Feb 15). PMCID: PMC3478770.
12. Sevin Turcan, Daniel Rohle, Anuj Goenka, Logan A. Walsh, Fang Fang, Emrullah Yilmaz, Carl Campos, Armida W.M. Fabius, Chao Lu, Patrick S. Ward, Craig B. Thompson, Andrew Kaufman, Olga Guryanova, Ross Levine, Adriana Heguy, Agnes Viale, Luc G.T. Morris, Jason T. Huse, Ingo K. Mellinghoff, and **Timothy A.**

Chan. (2012) IDH1 mutation is sufficient to establish the glioma hypermethylator phenotype. **Nature** (Feb 15) PMCID: PMC3351699.

13. Morris LGT, Kaufman AM, Gong Y, Ramaswami R, Walsh LA, Turcan S, Eng S, Kannan K, Zou Y, Peng L, Banuchi VE, Paty P, Zeng Z, Vakiani E, Solit D, Singh B, Ganly G, Liau L, Cloughesy TC, Mischel PS, Mellinghoff IM, **Chan TA.** (2013) Recurrent somatic mutation of FAT1 in multiple human cancers leads to aberrant Wnt activation. **Nature Genetics** (Jan 27) PMID: 23354438.
14. Ho AS, Kannan K, Roy DM, Morris LGT, Ganly I, Katabi N, Ramaswami D, Walsh LA, Eng S, Huse JT, Zhang J, Dolgalev I, Huberman K, Heguy A, Viale A, Drobnjak M, Leversha MA, Rice CE, Singh B, Iyer NG, Leemans CR, Bloemena E, Ferris RL, Seethala RR, Gross BE, Liang Y, Sinha R, Peng L, Raphael BJ, Turcan S, Gong Y, Schultz N, Kim S, Chiosea S, Shah JP, Sander C, Lee W, **Chan TA** (2013) The mutational landscape of adenoid cystic carcinoma. **Nature Genetics** (May 19) PMCID: PMC3708595.
15. Gong Y, Zack TI, Morris LGT, Lin K, Hukkelhoven E, Raheja R, Veeriah S, Meng S, Viale A, Schumacher SE, Beroukhim R, and **Chan TA**. (2014) Pan-cancer genetic analysis identifies PARK2 as a master regulator of G1/S cyclins. **Nature Genetics** (May 4) PMID: 24793136.

D. Research Support

Ongoing Research Support (selected due to space)

NIH/NCI RO1-154767A1, **Chan (PI)** 7/2011-7/2016
Elucidating the function of the widely inactivated phosphatase PTPRD in the molecular pathogenesis of glioblastoma
Role: PI
Aim is to determine the molecular mechanisms of PTPRD tumor suppression in GBM.

NIH R21DE23229-01, Chan (PI) 9/2012-9/2014
The mutational landscapes underlying aggressiveness in adenoid cystic carcinoma.
Role: PI
Aim is to determine the exonic mutations underlying tumor aggressiveness in adenoid cystic carcinoma.

2010TC, Chan (PI) 10/1/2010-9/30/2014
Sontag Foundation
Dissecting and Targeting the PTPRD/STAT3 Axis in Glioma
Role: PI
Aim is to evaluate the STAT3 signaling cascade in GBM and to develop strategies to target this in gliomas.

Era of Hope Award, Chan (PI) 5/2013-6/2018
Congressionally Directed Medical Research Programs
Department of Defense (DOD)
Role: PI
Aim is to characterize master regulators of breast cancer metastasis.

Completed Research Support

AVON Foundation Research Grant, Chan (PI) 12/2010-12/2012
Clinical impact of genomic biomarkers for recurrence.
Role: PI
Aim is to identify genomic biomarkers for recurrence in breast cancer patients.

Metastasis Research Center Grant, Chan (PI) 10/2010-10/2012
Large-scale analysis of the breast cancer epigenome
Role: PI
Aim is to use next-generation sequencing technologies to identify biomarkers for breast cancer metastasis.

Oncogene (2014), 1–15

www.nature.com/onc

ORIGINAL ARTICLE

RECK controls breast cancer metastasis by modulating a convergent, STAT3-dependent neoangiogenic switch

LA Walsh[1], DM Roy[1,2], M Reyngold[3], D Giri[4], A Snyder[1,5], S Turcan[1], CR Badwe[6], J Lyman[7], J Bromberg[5], TA King[7] and TA Chan[1,3]

Metastasis is the primary cause of cancer-related death in oncology patients. A comprehensive understanding of the molecular mechanisms that cancer cells usurp to promote metastatic dissemination is critical for the development and implementation of novel diagnostic and treatment strategies. Here we show that the membrane protein RECK (Reversion-inducing cysteine-rich protein with kazal motifs) controls breast cancer metastasis by modulating a novel, non-canonical and convergent signal transducer and activator of transcription factor 3 (STAT3)-dependent angiogenic program. Neoangiogenesis and STAT3 hyperactivation are known to be fundamentally important for metastasis, but the root molecular initiators of these phenotypes are poorly understood. Our study identifies loss of RECK as a critical and previously unknown trigger for these hallmarks of metastasis. Using multiple xenograft mouse models, we comprehensively show that RECK inhibits metastasis, concomitant with a suppression of neoangiogenesis at secondary sites, while leaving primary tumor growth unaffected. Further, with functional genomics and biochemical dissection we demonstrate that RECK controls this angiogenic rheostat through a novel complex with cell surface receptors to regulate STAT3 activation, cytokine signaling, and the induction of both vascular endothelial growth factor and urokinase plasminogen activator. In accordance with these findings, inhibition of STAT3 can rescue this phenotype both *in vitro* and *in vivo*. Taken together, our study uncovers, for the first time, that RECK is a novel regulator of multiple well-established and robust mediators of metastasis; thus, RECK is a keystone protein that may be exploited in a clinical setting to target metastatic disease from multiple angles.

Oncogene advance online publication, 16 June 2014; doi:10.1038/onc.2014.175

INTRODUCTION

Breast cancer is one of the most common cancers among women, causing over 400 000 deaths annually worldwide.[1] Metastatic disease is a major cause of morbidity and mortality and is currently incurable, making it a primary obstacle to improving breast cancer outcomes.[2] The molecular basis of metastasis remains incompletely understood. In recent years, a number of metastasis-suppressor genes (MSGs) have been discovered. These genes are defined by their specific ability to inhibit metastasis without altering primary tumor growth. Both preclinical models and retrospective human studies suggest that MSGs have key roles in controlling the development of metastasis.[3] Elucidating the molecular mechanisms by which these genes control the metastatic process offers valuable insight into tumor biology and may lead to new therapeutic options.

Reversion-inducing cysteine-rich protein with kazal motifs (RECK) is a putative MSG that is implicated in tumor progression.[4] RECK is a membrane-anchored protein that is involved in several physiological processes, including regulation of extracellular matrix (ECM) integrity, vascular growth during development and stabilization of tissue architecture.[5,6] In some cell systems, RECK can influence matrix metalloproteinase (MMP) function.[7] RECK expression is frequently silenced in tumor cells.[8,9] Interestingly, a recent study focusing on genome-wide DNA methylation profiling of CpG islands in breast cancer identified the RECK gene as a common target of promoter hypermethylation.[10] Despite documented effects of RECK on the behavior of tumor cells, the signaling pathways targeted by RECK and the specific mechanism by which RECK modulates metastasis remain elusive. Furthermore, while RECK-mediated invasion has been largely attributed to changes in MMP expression *in vitro*, most tumors and tumor cell lines express extremely low levels of MMPs, suggesting that additional mechanisms are likely at play.[11,12]

In this study, we apply a systematic, multifaceted strategy using human tumor samples, *in vivo* metastasis models and multiple, unbiased high throughput analyses to provide a comprehensive analysis of the role of RECK during breast cancer metastasis. We generated new data sets that include large number of patient samples and used them to illustrate a relationship between RECK expression and disease-specific survival. Furthermore, analyses of matched pairs of primary human breast tumors and distant metastases reveal that RECK expression is further silenced during metastatic progression. We demonstrate using multiple mouse models that RECK reconstitution *in vivo* suppresses tumor metastases. Using several unbiased screens, we have identified novel pathways and binding partners that directly mediate the effects of RECK on metastasis. Finally, we show that RECK controls these phenotypes through signal transducer and activator of transcription factor 3 (STAT3)-dependent regulation of an angiogenic program.

[1]Human Oncology and Pathogenesis Program, Memorial Sloan-Kettering Cancer Center, New York, NY, USA; [2]Weill Cornell Rockefeller/Sloan-Kettering Tri-Institutional MD-PhD Program, New York, NY, USA; [3]Department of Radiation Oncology, Memorial Sloan-Kettering Cancer Center, New York, NY, USA; [4]Department of Pathology, Memorial Sloan-Kettering Cancer Center, New York, NY, USA; [5]Department of Medicine, Memorial Sloan-Kettering Cancer Center, New York, NY, USA; [6]Weill Graduate School of Medical Sciences, New York, NY, USA and [7]Department of Surgery, Memorial Sloan-Kettering Cancer Center, New York, NY, USA. Correspondence: Dr TA Chan, Human Oncology and Pathogenesis Program, Memorial Sloan-Kettering Cancer Center, 1275 York Avenue, Box 20, New York, NY 10065, USA.
E-mail: chant@mskcc.org
Received 28 February 2014; revised 30 April 2014; accepted 9 May 2014

RESULTS

Analysis of matched lymph node and distant metastases demonstrates that RECK expression is downregulated during metastatic breast cancer progression

We first sought to explore whether RECK expression was lost specifically during metastatic progression or whether the process of RECK silencing was already completed in the primary tumor. To answer this question, we first evaluated RECK gene expression in 36 primary tumors and lymph node metastasis pairs. Microarray analysis of these tumors revealed a significant decrease in RECK expression in metastatic lymph nodes compared with matched primary tumors in luminal A, luminal B and Her 2 subytpes ($P = 0.0009$, Figure 1a). These results were confirmed by qunatitative reverse transcriptase–PCR (qRT–PCR; $P < 0.01$, Supplementary Figure S1A). Interestingly, we did not see a significant difference in RECK expression in the basal subtype (Figure 1a); however, the baseline expression of RECK in our basal primary tumors was already considerably lower than other subtypes (Supplementary Figure S1B). This is not seen with other larger patient cohorts, suggesting that there may be significant diversity in RECK expression between different basal tumors.

We next wanted to determine whether the RECK silencing was also evident in distant metastases. We performed immunohistochemistry (IHC) for RECK on 43 matched primary breast tumors and distant metastatic lesions (including the lung, liver and bone) and scored the staining intensity. Distant metastases had significantly decreased RECK expression compared with matched primary tumors ($P = 0.001$, Figure 1b, Supplementary Figure S1C and D). Together, these data show that RECK expression is lost in many tumors during progression from primary tumor to metastasis, consistent with a role for RECK in protecting against metastatic breast cancer.

RECK does not alter cell proliferation and loss of RECK alone is not sufficient to achieve cellular transformation

As RECK expression is low in most solid tumor cell lines, we next investigated the effects of reconstituting RECK expression (by constitutively expressing RECK via lentiviral transduction) in three highly invasive breast cancer cell lines (MDA-MB-231, LM2-4175 and BOM1-1833). RECK expression was confirmed by western blotting (Figure 2a), and proper membrane localization was visualized by immunocytochemistry and confocal microscopy (Figure 2b). Altered RECK expression did not change the rate of cell growth *in vitro* (Figures 2c–e) nor did it result in cell cycle changes (Figures 2f–h). Given that RECK expression is lower in clinical tumor specimens compared with normal breast tissue, we next sought to examine whether loss of RECK is sufficient for malignant transformation. Stable knockdown of RECK did not transform normal human mammary epithelial cells (HMECs) in xenograft assays (Figures 2i–k). These results suggest that RECK loss is not sufficient to result in transformation or altered cell division but instead may act via other mechanisms.

RECK suppresses vascular endothelial growth factor (VEGF) expression, endothelial recruitment in metastatic lesions and metastatic burden *in vivo*

We next examined whether reconstituting RECK could reduce metastatic burden in an *in vivo* model of metastasis. Accordingly, we stably expressed RECK in LM2-4175 cells (an *in vivo* selected and highly lung metastatic cell line)[13,14] and injected them into the lateral tail vein of athymic nude mice. Bioluminescent imaging (BLI) of mice re-expressing RECK revealed a significant decrease in metastatic tumor burden compared with empty vector (EV) control (Figures 3a and b). Given that a significant difference in metastatic burden was first evident via BLI at 4 weeks post-intravenous injection (Figure 3b), we harvested lung tissue from each group at this time point for detailed analysis. Consistent with the BLI data at 4 weeks, hematoxylin and eosin (H&E) staining of lung tissue (Figure 3c) revealed a significant decrease in tumor burden (Figure 3d) and the number of metastatic foci (Figure 3e) in mice injected with cells re-expressing RECK.

RECK has been previously suggested to have a role in vascular organization.[7] Therefore, we stained lung tissue for CD34 and VEGF. RECK-expressing metastatic foci had significantly less CD34 staining (Figures 3c and f), suggesting that RECK suppresses *de novo* blood vessel formation or recruitment. This phenotype was concomitant with decreased VEGF (Figures 3c and g) and Ki67 expression (Figures 3c and h), demonstrating that RECK may interfere with metastatic outgrowth by reducing vascularization. A decrease in metastasis *in vivo* was also observed after intracardiac injection of BOM1-1833 cells (an *in vivo* selected and highly bone metastatic cell line)[13] re-expressing RECK (Figures 3i and j).

RECK has been hypothesized to act in part through MMP-2, MMP-9 and MT1-MMP in some cell systems.[15–17] Interestingly, in our breast metastatic model, immunostaining of metastatic nodules for MMP2- MMP-9 and MT1-MMP revealed no significant changes in expression (Supplementary Figure S2A–C). However, as immunostaining does not discriminate between latent and active MMP-2 and MMP-9, we cannot discount the possibility that there may be differences in MMP activity. Nevertheless, MMP-2 and MMP-9 were undetectable in conditioned media from MDA-MB-231, LM2-4175 and BOM1-1833 by enzyme-linked immunosorbent assay (ELISA; data not shown), suggesting that any differences seen *in vivo* are likely from changes in secretion of these proteins from surrounding stroma and not from the tumor cells themselves. Together, these data suggest that the phenotypic effects of RECK expression in breast cancer metastases may involve novel mechanisms independent of MMPs.

Coordinate control of a cooperative neovascularization program by RECK via regulation of endothelial remodeling and multiple secreted regulators of angiogenesis

In order to gain further insight into the molecular changes associated with RECK expression, we analyzed the transcriptomes of MDA-MB-231 and LM2-4175 cells overexpressing RECK. Ingenuity pathway analysis of differentially expressed genes between control and RECK-overexpressing cells (Supplementary Tables S1 and S2) revealed significant alterations in IL-6, IL-8 and IL-10 signaling pathways in both cell lines (Figures 4a and b, Supplementary Tables S5 and S6). In addition, VEGF and hypoxia-inducible factor-1α signaling pathways were also altered in MDA-MB-231 and LM2-4175 cells, respectively. All of these pathways are intimately involved in the regulation of angiogenesis, consistent with our hypothesis that RECK can control transcriptional programs that influence tumor neovascularization.[18–20]

We next asked whether reconstituting RECK was sufficient to alter VEGF secretion or endothelial cell phenotypes *in vitro*. ELISAs were performed on conditioned media from MDA-MB-231, LM2-4175 and BOM1-1833 cells re-expressing RECK, and all were found to secrete significantly less VEGF compared with their respective controls (Figure 4c). In addition, conditioned media from MDA-MB-231 and LM2-4175 cells re-expressing RECK inhibited chemotaxis of endothelial cells using Boyden transwell assays (Figures 4d and e). Importantly, this phenotype was rescued with the addition of recombinant VEGF. Furthermore, conditioned media from MDA-MB-231 and LM2-4175 cells re-expressing RECK significantly reduced endothelial cell tube formation *in vitro* (Figures 4f and g), showing that RECK can regulate endothelial organization. These data suggest that RECK may be an important modulator of tumor-mediated angiogenesis, consistent with the changes observed *in vivo*.

To determine whether there are other potential angiogenic factors besides VEGF that are altered by RECK, we performed an

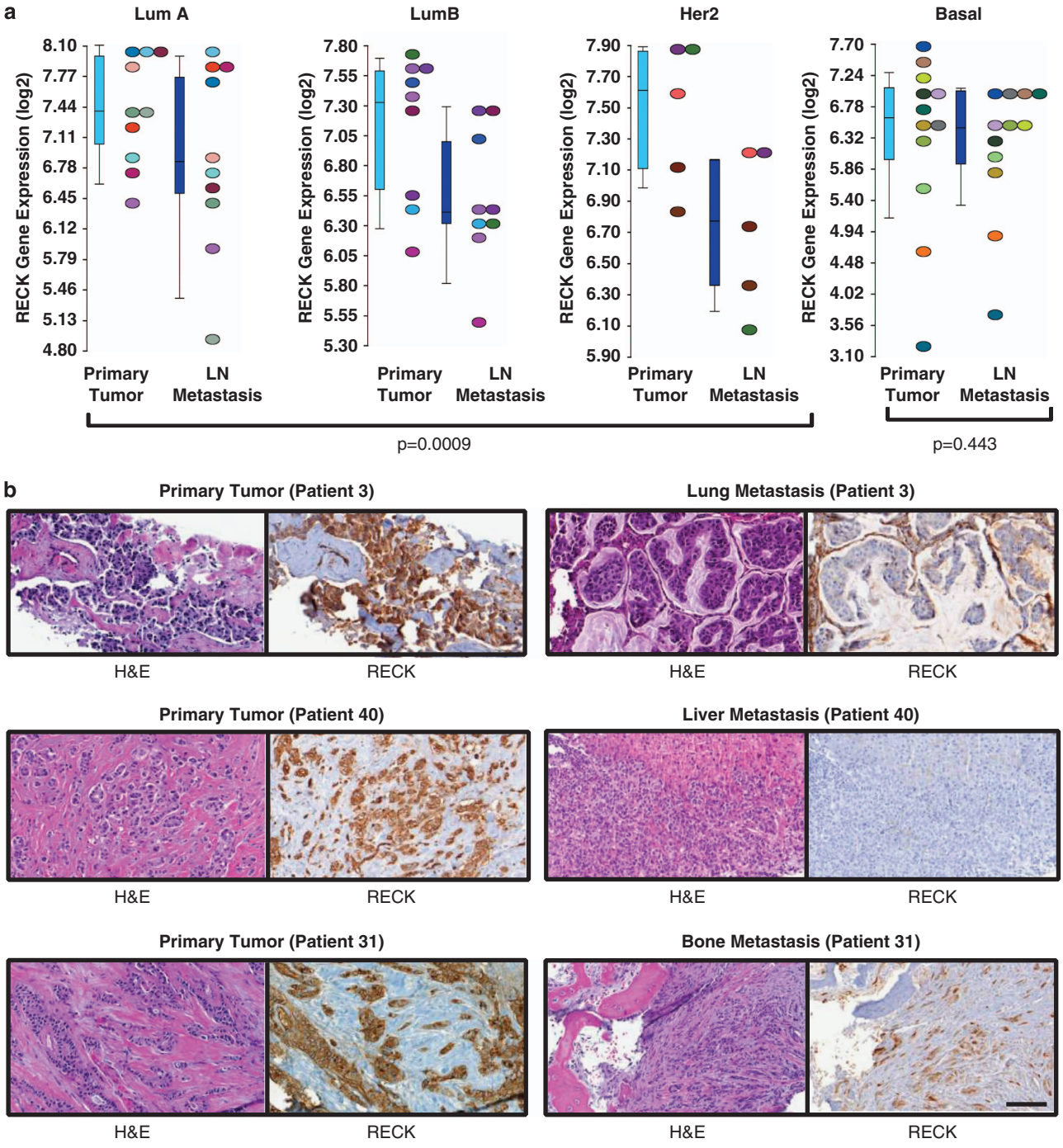

Figure 1. Analyses of matched pairs demonstrates that RECK is downregulated during metastatic progression in both lymph nodes and distant sites. (**a**) RECK is silenced during the establishment of nodal metastases. Expression levels of RECK in 36 matched pairs of primary breast tumors and lymph node metastases segregated based on PAM50 subtype (LumA, LumB, Her2 together ($P = 0.0009$); LumA ($P = 0.4609$), LumB ($P = 0.0078$), Her2 ($P = 0.125$) and Basal ($P = 0.443$). Wilcoxon matched-pairs signed rank test. Data are from microarray analysis. (**b**) RECK is silenced in distant metastases. Representative images of H&E staining and RECK IHC of matched primary breast tumors and distant metastases. RECK staining was scored and statistical quantification was based on Wilcoxon matched-pairs signed rank test ($P = 0.001$, $n = 43$).

antibody array screen of 55 known pro- or anti-angiogenic factors, including various ECM components, proteases, growth factors and signaling molecules. LM2-4175 cells expressing either RECK or EV were subject to a low oxygen challenge (0.5% O_2) to mimic the hypoxic tumor environment and stimulate release of angiogenic factors. After 24 h, conditioned media was isolated from both cell lines and screened with the array. Strikingly, the array revealed that reconstituting RECK coordinately suppressed many pro-angiogenic factors and increased the secretion of anti-angiogenic factors (Figures 4h and i). For example, reconstituting RECK potently suppressed the secretion of urokinase plasminogen activator (uPA), a major modulator of extracellular proteolysis and angiogenesis and a known mediator of breast cancer metastasis.[21] We confirmed RECK-mediated suppression of uPA secretion by ELISA in three breast cancer cell lines (Figure 4j). Together these data demonstrate an important role for RECK in coordinately

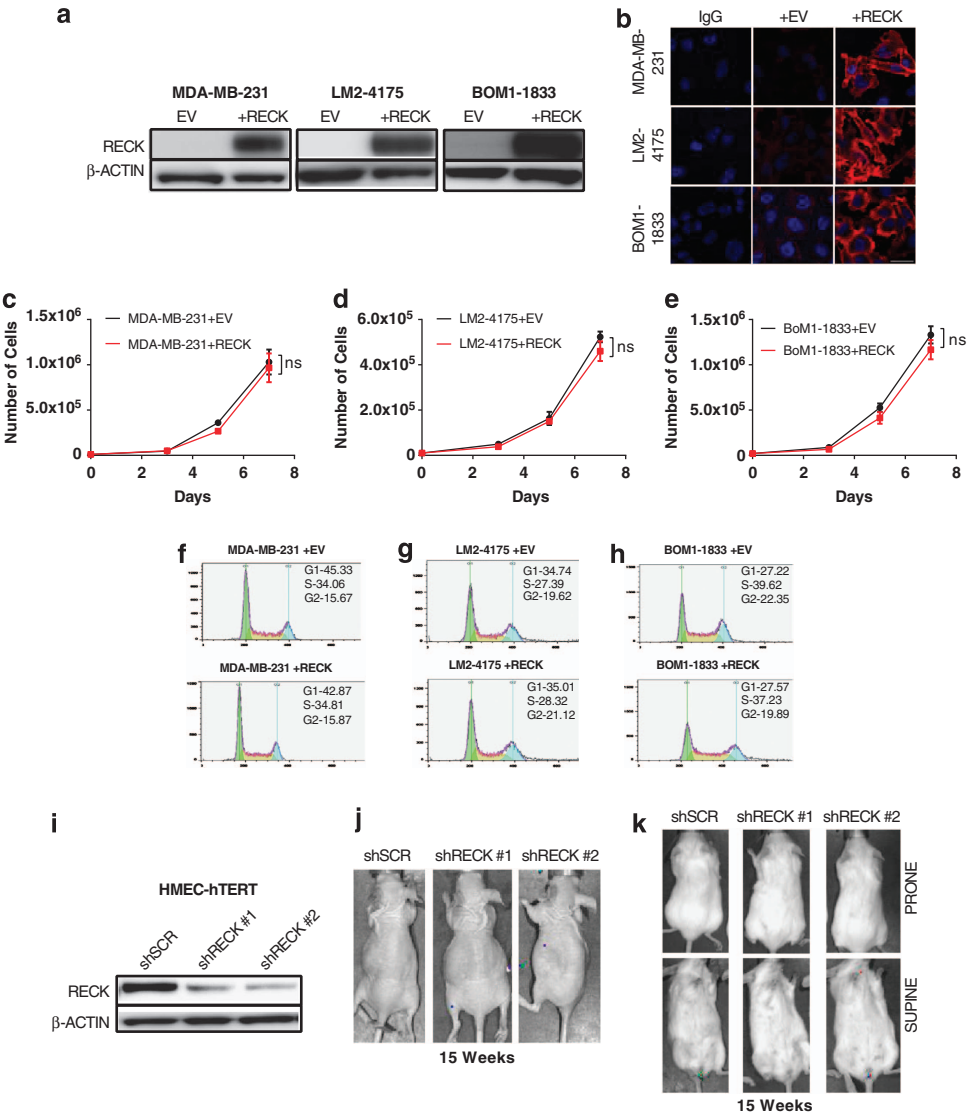

Figure 2. RECK does not affect cell cycle or growth rate in invasive breast cancer cells and loss of RECK alone is insufficient to transform cells. (**a**) Overexpression of RECK in breast cancer cell lines. Representative western blotting analysis of MDA-MB-231, LM2-4175 and BOM1-1833 cells stably transduced with the lentiviral constructs indicated. β-Actin was used as a loading control. (**b**) Representative confocal immunofluorescent images of MDA-MB-231, LM2-4175 and BOM1-1833 cells stably transduced with lentiviral constructs indicated. IgG was used as a staining control. Scale bar represent 20 μM. Growth curve of (**c**) MDA-MB-231 (**d**) LM2-4175 and (**e**) BOM1-1833 cells stably transduced with lentiviral constructs. Data are presented as mean ± s.e.m. ($n = 3$). Flow cytometric cell cycle analysis of (**f**) MDA-MB-231 (**g**) LM2-4175 and (**h**) BOM1-1833 cells stably transduced with lentiviral constructs indicated. Cell cycle curves and quantification of stages of cell cycle was based on the Watson (pragmatic) model ($n > 10\,000$ events). (**i**) Representative immunoblot of HMEC-hTERT stably infected with the lentivirus indicated. HMEC-hTERT stably infected with the indicated lentiviral constructs were injected into the (**j**) lateral tail vein of of athymic nude mice ($n = 5$) or (**k**) the mammary fat pad of NSG mice ($n = 5$). Representative BLI images at 15 weeks postinjection are shown.

modulating multiple angiogenic factors and for the first time reveal a link between RECK and regulation of uPA.

A spontaneous metastasis assay reveals that RECK suppresses metastasis in part through negative regulation of uPA

Given our finding that RECK modulates the secretion of uPA, a well-documented protein involved in ECM proteolysis and breast cancer metastasis, we next wanted to determine whether reconstituting RECK in breast cancer cells could suppress spontaneous metastasis *in vivo*. Metastasis is a multistep process, including initial invasion of surrounding tissue, intravasation/extravasation and survival and outgrowth at secondary sites.[22] Although frequently modeled using tail vein injection, metastasis modeled via orthotopic injection may more accurately recapitulate the steps necessary for metastasis. MDA-MB-231 cells expressing either EV or RECK were orthotopically injected into the mammary fat pad of NOD/SCID/IL2Rγ-deficient (NSG) mice. Consistent with our *in vitro* proliferation results, primary tumor volume was unchanged following RECK re-expression (Figure 5a). BLI of mice at day 40 revealed a significant decrease in spontaneous metastasis from tumors expressing high RECK vs control (Figures 5b and c), which was confirmed by H&E staining and quantification of tumor burden in the lung and liver (Figures 5d and e). IHC was used to confirm that RECK expression was high in primary tumors with reconstituted RECK at day 40 (Figure 5f). Furthermore, IHC for uPA in primary tumors re-expressing RECK revealed a significant decrease in uPA staining intensity compared with controls (Figure 5g), again suggesting a strong relationship between RECK, uPA and metastasis.

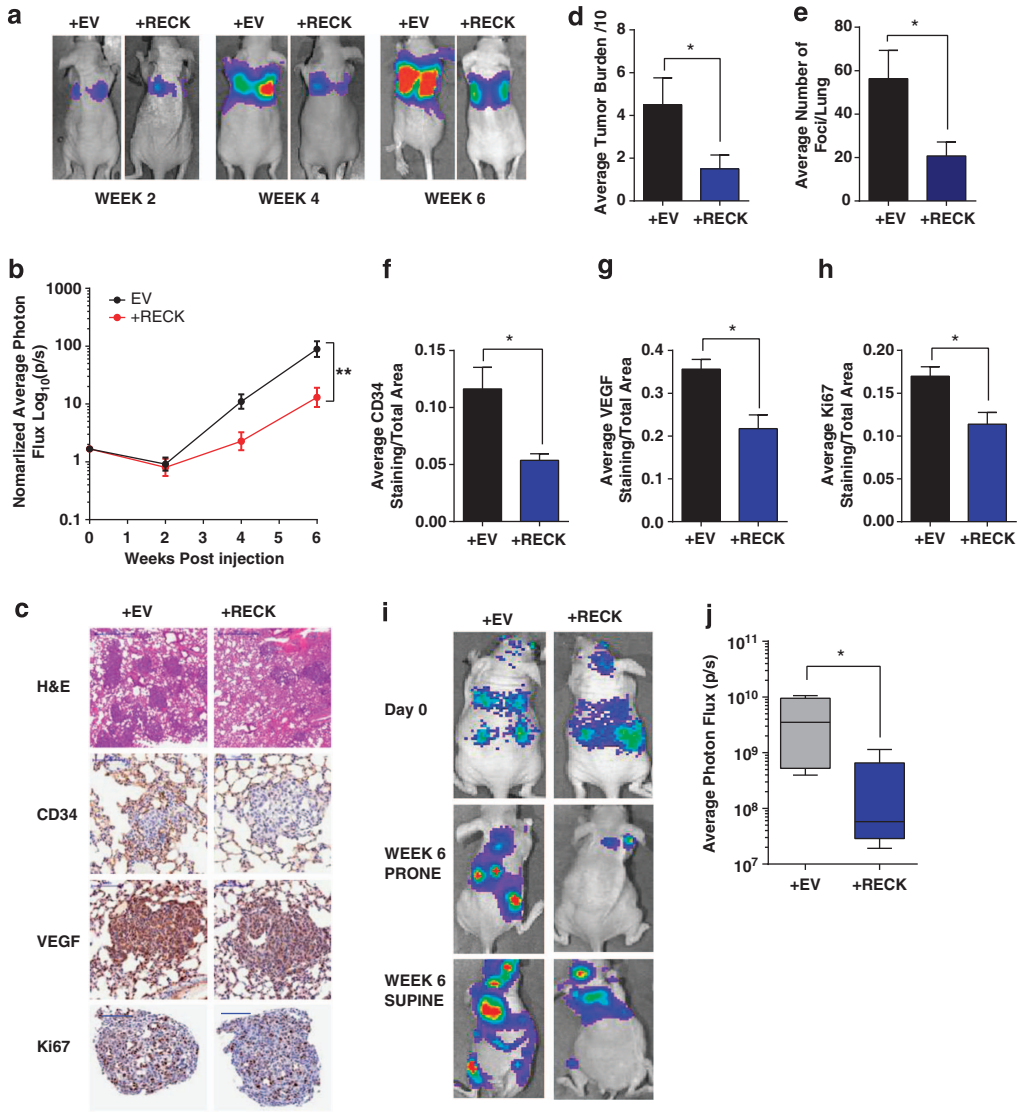

Figure 3. Reconstituting RECK in breast cancer cells results in decreased VEGF, vascular recruitment and metastatic burden *in vivo*. LM2-4175 +EV or LM2-4175+RECK cells were injected into the lateral tail vein of athymic nude mice ($n \geqslant 7$). BLI images were taken over a period of 6 weeks. (**a**) Representative images are depicted. (**b**) Graph of BLI quantification over time. Data are presented as mean ± s.e.m. (**$P < 0.01$). (**c**) Mice were killed at 4 weeks, and lung tissue was stained with H&E, CD34, VEGF and Ki67. Scale bars represent 500, 100, 100 and 100 μm, respectively. (**d**) Scoring of metastatic tumor burden in H&E-stained lungs. Data are presented as mean ± s.e.m. (*$P < 0.05$, $n \geqslant 3$). (**e**) Quantification of average number of metastatic foci per lung. Data are presented as mean ± s.e.m. (*$P < 0.05$, $n \geqslant 3$). Quantification of (**f**) CD34, (**g**) VEGF and (**h**) Ki67 staining. Data are presented as mean ± s.e.m. (*$P < 0.05$, $n \geqslant 3$). BOM1-1833+EV or BOM1-1833+RECK cells were intracardiac injected into the left ventricle of athymic nude mice ($n = 5$). (**i**) Representative BLI of mice 6 weeks postinjection. (**j**) Quantification of BLI at 6 weeks postinjection. Data are presented as whisker box plots (*$P < 0.05$, $n = 5$).

Depletion of RECK promotes a uPA-dependent invasion and pro-angiogenic program

To evaluate the effect of RECK perturbation on VEGF and uPA, we knocked down RECK in the breast cancer cell lines Hs343T and Hs606T. We chose these cell lines as they have significant endogenous levels of RECK expression (Cancer Cell Line Encyclopedia, Broad, Supplementary Figure S3). Hs343T and Hs606T cells were transfected with scramble (control) or RECK small interfering RNA (siRNA). RECK knockdown was confirmed by western blotting (Figure 6a). Consistent with our RECK re-expression experiments, RECK knockdown had no significant effect on the growth of cells. Representative growth curves from Hs606T cells are shown in Figure 6b. ELISA performed on conditioned media isolated from these cells demonstrated that RECK knockdown results in a significant increase in VEGF and uPA secretion (Figures 6c and e). These changes were concurrent with changes in *VEGF* and *PLAU* gene expression (Figures 6d and f). Furthermore, using a Matrigel transwell invasion assay, we revealed that RECK knockdown significantly increased invasion of both Hs343T and Hs606T lines and that this was rescued by concomitant knockdown of uPA (siPLAU Figures 6g and h). This suggests that the increased invasive potential associated with the loss of RECK could be, in part, due to increases in uPA secretion. Finally, to test the effects of RECK loss on angiogenic markers, we repeated the angiogenesis protein array using conditioned media from Hs606T cells transfected with either scramble (control) or RECK siRNA. Consistent with previous results, RECK knockdown resulted in high levels of pro-angiogenic factors in conditioned media, including VEGF and uPA, and reduced levels of anti-angiogenic factors (Figures 6i and j).

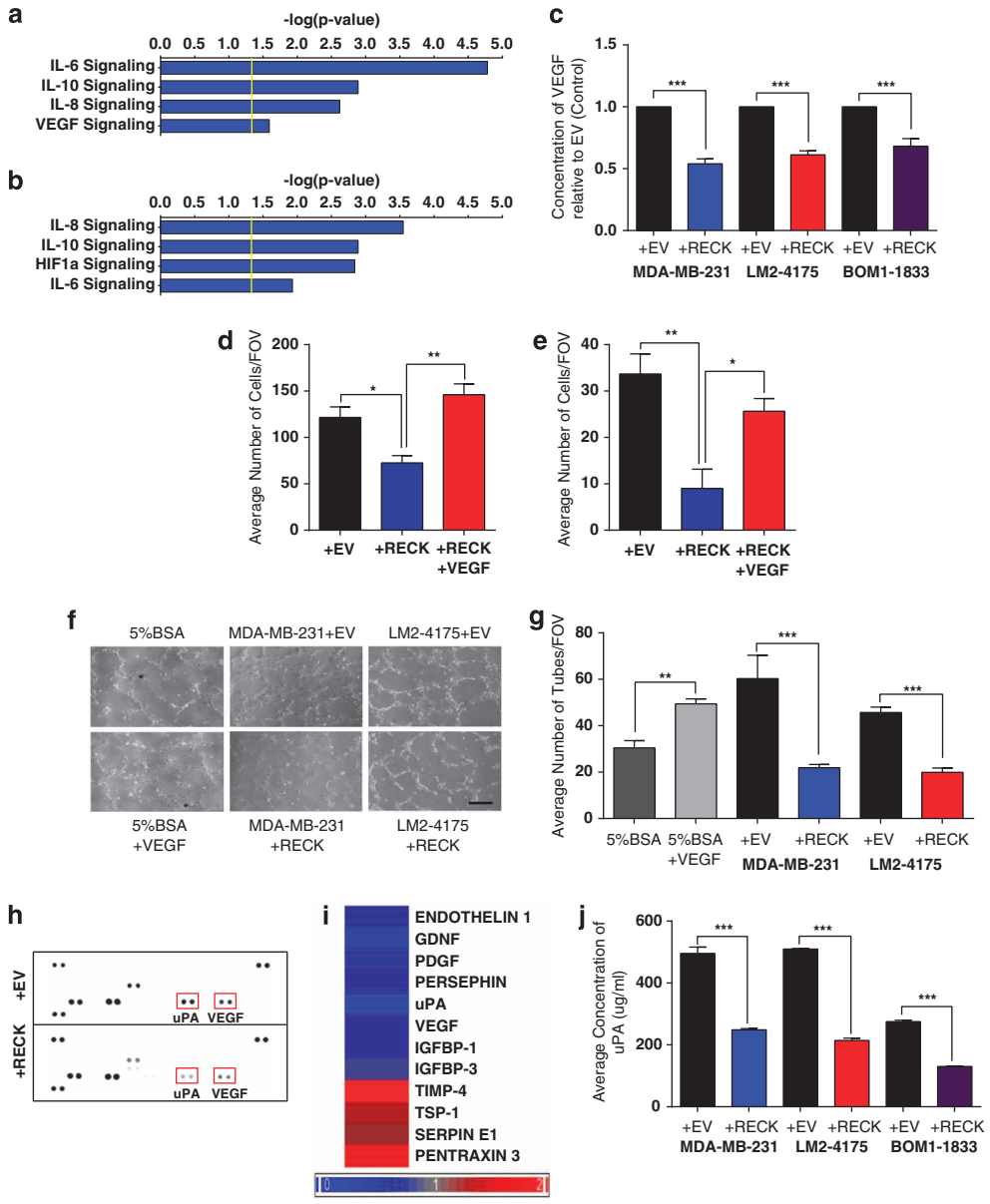

Figure 4. RECK regulates angiogenic and cytokine transcriptional programs, endothelial reorganization and a neovascular switch. RECK expression resulted in significant changes in IL-6, IL-10, IL-8, HIF1a and VEGF pathway genes. U133A 2.0 expression arrays were used to compare the transcriptomes of (**a**) MDA-MB-231+EV and MDA-MB-231+RECK cells or (**b**) LM2-4175+EV and LM2-4175+RECK cells. Differentially expressed genes were analyzed using the IPA software. (**c**) ELISA was used to determine VEGF concentrations in conditioned media from MDA-MB-231, LM2-4175 and BOM1-1833 cells stably transduced with lentiviral constructs indicated. Data are presented as mean ± s.e.m. (***$P < 0.001$, $n = 3$). (**d**) RECK suppresses endothelial cell migration, which is rescued by VEGF. Conditioned media from MDA-MB-231+EV, MDA-MB-231+RECK or MDA-MB-231+RECK+10 μM recombinant VEGF was used as a chemoattractant for HUVEC cells in a Boyden transwell chamber migration assay. Data are presented as mean ± s.e.m. (*$P < 0.05$, **$P < 0.01$, $n = 4$). (**e**) Same as in panel (**d**) but with LM2-4175 cells (*$P < 0.05$, **$P < 0.01$, $n = 4$). (**f**) RECK regulates endothelial cell reorganization. Conditioned media from MDA-MB-231 or LM2-4175 cells stably transduced with the indicated lentiviral constructs was used to resuspend HUVEC cells in an *in vitro* tube formation assay. 5% BSA and 5% BSA +10 μM recombinant VEGF were used as negative and positive controls, respectively. Representative images are shown in panel (**f**). Scale bars represent 200 μm. (**g**) Quantification of tube formation data are presented as mean ± s.e.m. (***$P < 0.001$, $n = 3$). (**h**) RECK regulates a coordinated, convergent angiogenic switch. LM2-4175+EV and LM2-4175+RECK were placed at 0.5% O_2 for 24 h. Conditioned media from these cells was used to probe an angiogenesis array. Protein expression was quantified by densitometry, and select candidates are shown in heat map (**i**). (**j**) ELISA was used to determine uPA concentrations in conditioned media from MDA-MB-231, LM2-4175 and BOM1-1833 cells stably transduced with the indicated lentiviral constructs. Data are presented as mean ± s.e.m. (***$P < 0.001$, $n = 3$).

RECK associates with multiple cell surface receptors, modulates cytokine signaling and activates STAT3 signaling

To further dissect the details of the signaling pathways that underlie the effects of RECK, we tested the results of RECK knockdown on global gene expression in Hs343T and Hs606T cells (Supplementary Tables S3 and S4). Microarray and ingenuity pathway analysis analyses revealed that IL-6, IL-8, L10 and Janus-activated kinase/STAT signaling pathways were significantly altered in response to RECK knockdown in both the cell lines tested (Figures 7a and b, Supplementary Tables S7 and S8).

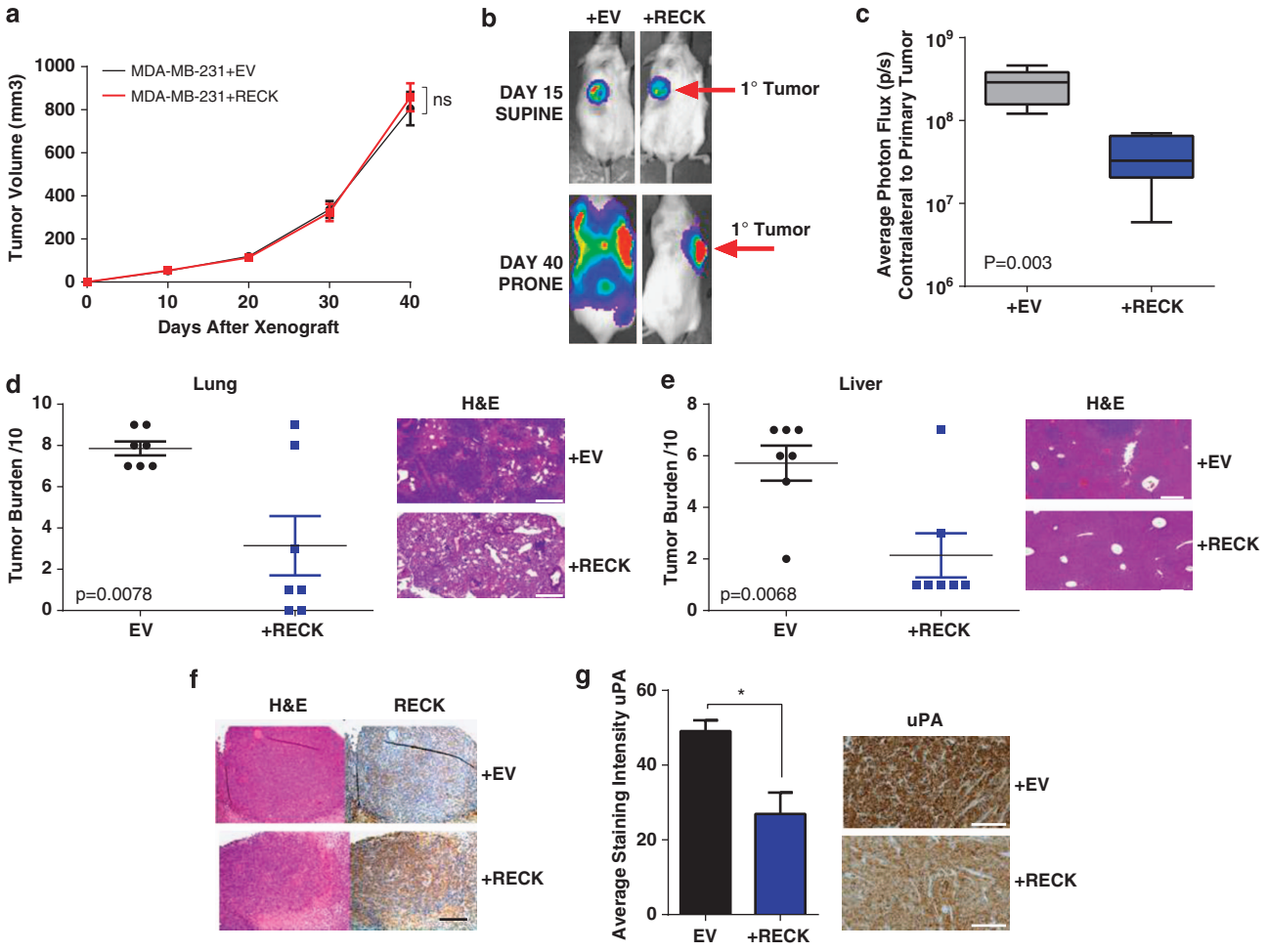

Figure 5. Orthotopic metastasis model demonstrates that RECK decreases lung and liver metastasis but does not significantly alter growth of the primary tumor. MDA-MB-231+EV and MDA-MB-231+RECK cells were injected into the mammary fat pad of NSG mice. (**a**) Quantification of primary tumor volume over time. Data are presented as mean ± s.e.m. (NS = not significant, $n = 7$). (**b**) RECK suppresses metastatic dissemination in an orthotopic model. Representative BLI of mice at days 15 and 40. (**c**) Quantification of BLI on the contralateral side from primary tumor at day 40. Data are presented as whiskers min. to max. ($P = 0.003$, $n = 7$). Lung and liver tissue was isolated from mice at day 40 and were sectioned and stained with H&E. Representative H&E sections and quantification of metastatic tumor burden are shown for both (**d**) lung and (**e**) liver. Scale bars represent 300 μm. Data are presented as mean ± s.e.m. ($n = 7$). (**f**) Representative image of primary tumors stained with H&E and IHC for RECK. Data are presented as mean ± s.e.m.. Scale bars represent 200 μm. (**g**) RECK expression suppresses uPA. Representative IHC of primary tumors for uPA and quantification of staining intensity. Scale bars represent 150 μm. Quantification was performed using the MetaMorph software. Data are presented as mean ± s.e.m. (*$P < 0.05$, $n \geqslant 4$).

Importantly, these data are consistent with pathways altered by reconstituting RECK in previous experiments (Figures 4a and b, Supplementary Tables S1).

Given that RECK is a glycosylphosphatidylinisotol-anchored membrane protein, we hypothesized that RECK may be altering signaling pathways by directly binding other membrane proteins, extracellular cytokines or proteases. To test this, we modified a receptor antibody array to screen for potential RECK binding partners. RECK-immunoprecipitated lysate from Hs606T cells was used to probe a panel of 119 soluble extracellular or membrane-bound proteins. Immunoprecipitation revealed that RECK bound to IL-8, β1-integrin and galectin-1 (Figure 7c). As a positive control, we confirmed RECK binding in this modified system and by conventional western blotting (Figures 7c and d). We validated the interaction screen by immunoblot for β1-integrin and galectin-1 (Figure 7d). As one of the most significantly altered pathways common to all microarray analysis was IL-6 signaling, we next determined that RECK also directly complexes with IL-6RA and gp130, the principle mechanism of IL-6 signaling in breast cancer (Figure 7d).[23] Finally, we identified that RECK also binds to the uPA receptor uPAR (Figure 7d), providing a possible additional mechanism for RECK-mediated suppression of uPA activity.

To characterize RECK-induced signaling events in the cytoplasm, we used a phospho-protein array and compared lysate from MDA-MB-231+EV and MDA-MB-231+RECK cells. RECK expression results in decreased phosphorylation of a number or growth-related oncoproteins. Among the most significantly downregulated phospho-proteins was pSTAT3. RECK expression resulted in a loss of phosphorylation on the activating Y705 residue (Supplementary Figure S4A). Interestingly, this is consistent with our protein and microarray results, as pSTAT3 is a well-described downstream effector of IL-6 and IL-8 and is capable of inducing both VEGF and uPA.[24–27] We confirmed that pSTAT3 is regulated by RECK using a doxycycline-inducible construct, showing that RECK induction resulted in significantly decreased pSTAT3 levels (Figure 7e). Furthermore, even under hypoxic conditions, which are known to potently activate STAT3 via phosphorylation,[28,29] pSTAT3 was suppressed upon RECK reconstitution in LM2-4175 cells (Figure 7f). Consistent with these data, knockdown of RECK with siRNA in Hs343T and Hs606T cells resulted in increased pSTAT3 (Figures 7g and h).

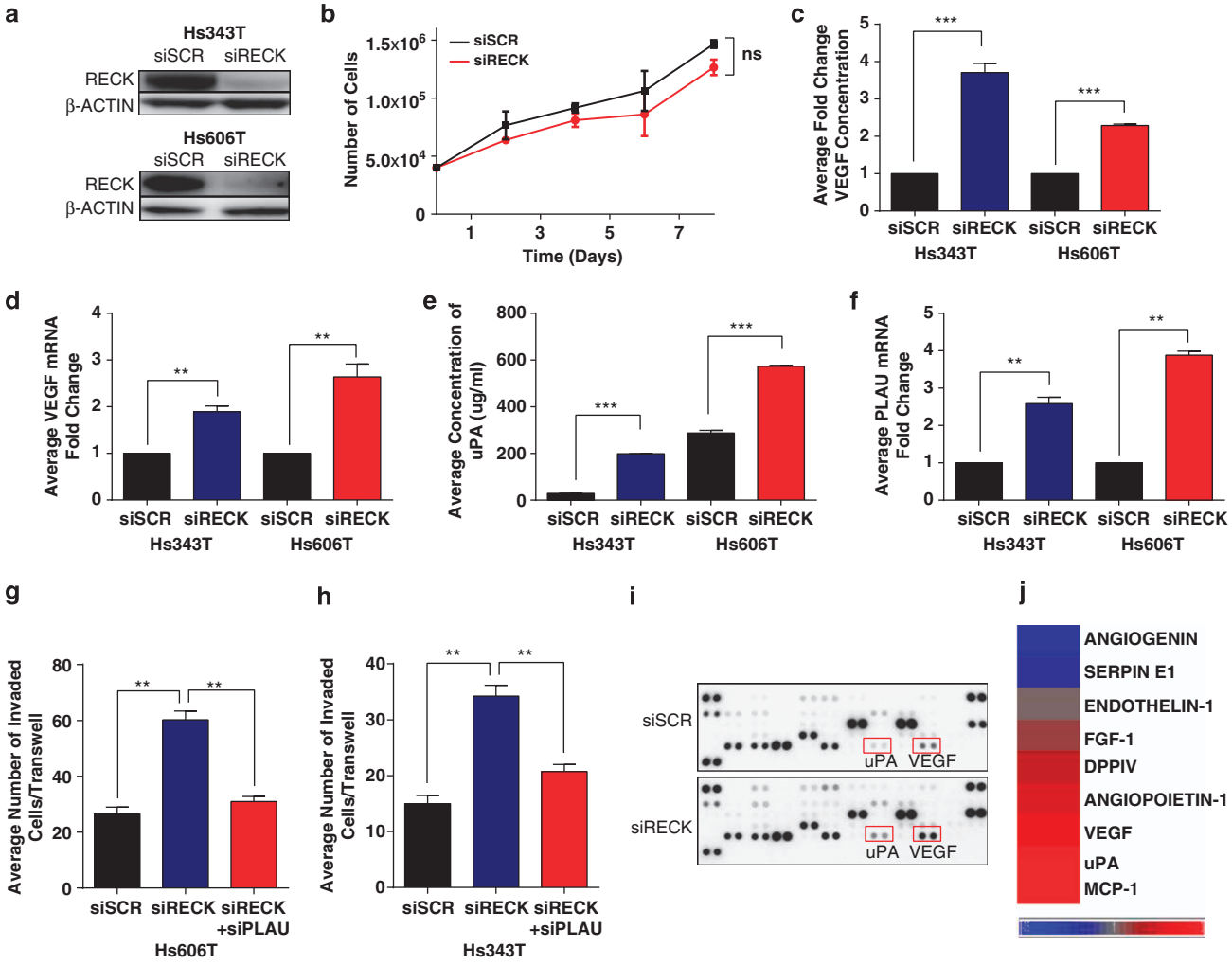

Figure 6. RECK depletion elevates VEGF and uPA secretion, activation of a coordinate pro-angiogenic program, and increases invasive potential but does not affect cell growth. (**a**) Representative immunoblot of Hs343T and Hs606T cells 48 h after transfection with SCR (scramble) or RECK siRNA. (**b**) Growth curve of Hs606T cells transfected with the indicated siRNA. Data are presented as mean ± s.e.m. (NS = not significant, $n = 3$). (**c**) VEGF ELISA on conditioned media isolated from Hs343T and Hs606T transfected with the indicated siRNA. Data are presented as mean ± s.e.m. (***$P < 0.001$, $n = 3$). (**d**) qRT–PCR of VEGF gene expression after transfection with the indicated siRNA. Data are presented as mean ± s.e.m. (**$P < 0.01$, $n = 3$). (**e**) uPA ELISA on conditioned media isolated from Hs343T and Hs606T transfected with the indicated siRNA. Data are presented as mean ± s.e.m. (***$P < 0.001$, $n = 3$). (**f**) qRT–PCR of PLAU gene expression after transfection with the indicated siRNA. Data are presented as mean ± s.e.m. (**$P < 0.01$, $n = 3$). Quantification of Boyden transwell invasion of (**g**) Hs343T and (**h**) Hs606T cells transfected with the indicated siRNAs. Data are presented as mean ± s.e.m. (***$P < 0.001$, $n \geqslant 3$). Conditioned media from Hs606T cells transfected with the indicated siRNA was used to probe an angiogenesis antibody array. (**i**) Image of array was used to quantify protein expression by densitometry, and altered candidates are shown in heat map (**j**).

Figure 7. RECK binds to multiple cell surface receptors and regulates cytokine and STAT3 signaling to modulate metastasis and survival. RECK knockdown resulted in significant changes in cytokine and angiogenesis pathways, including IL-6, IL-10, IL-8, Jak/Stat and VEGF. Human Genome U133A 2.0 expression arrays were used to compare the transcriptomes of (**a**) scramble vs siRECK in Hs343T cells and (**b**) scramble vs siRECK in Hs606T cells. Differentially expressed genes were analyzed using the IPA software. Immunoprecipitation using anti-RECK antibody in Hs606T cell lysate was used to probe a human soluble receptor antibody array. (**c**) Image of array highlighting enhanced RECK, IL-8, ITGB1 and GAL1 signal in IP-RECK compared with IgG (control). In the lower panel, data for each protein were taken at different exposures. (**d**) RECK binds to novel receptors that signal through STAT3. RECK co-IP demonstrates that RECK binds to β1-integrin, Galectin-1, IL-6Ra, gp130 and uPAR. (**e**) RECK decreases STAT3 activation. Representative immunoblot of lysates from MDA-MB-231 cells stably infected with a doxycyclin (dox)-inducible RECK plasmid. Cells were treated with 1 μg/ml dox for 18 h before harvesting lysate. Whole-cell lysate was used to probe for RECK, STAT3 and pSTAT3. β-Actin was used as a loading control. (**f**) RECK decreases STAT3 activation in hypoxic conditions. Representative immunoblot of LM2-4175 cells stably infected with lentiviral constructs indicated. Cells were placed in hypoxic conditions (0.5% O_2) for 24 h before harvesting lysates. RECK depletion increases pSTAT3 levels. Representative immunoblot analysis of (**g**) Hs343T and (**h**) Hs606T cells transfected with the indicated siRNA. (**i**) STAT3 knockdown reverses the increased invasion resulting from RECK depletion. Quantification of invasion of Hs606T cells transfected with indicated siRNAs. Data are presented as mean ± s.e.m. (*$P < 0.05$, $n = 3$). (**j**) STAT3 expression reverses increases in VEGF secretion post-RECK depletion. VEGF ELISA on conditioned media isolated from Hs606T cells transfected with indicated siRNA. Data are presented as mean ± s.e.m. (**$P < 0.01$, ***$P < 0.001$, $n = 3$). (**k**) STAT3 reverses RECK-dependent suppression of metastasis. LM2-4175+RECK, LM2-4175+STAT3 and LM2-4175+RECK+STAT3 cells were injected into the mammary fat pad of NSG mice. Quantification of BLI on the contralateral side of the primary tumor was performed on day 30. Data are presented as whisker box plots, with the line depicting the mean and the boxes showing 1 s.d. ($n = 5$). (**l**) Lungs were isolated, sectioned and stained with H&E, and the metastatic tumor burden was quantified out of 10. (**m**) Kaplan–Meier of mice injected via tail vein with cells described in panel (**k**). Increased survival conferred by RECK expression is reversed by concomitant overexpression of STAT3. $P = 0.023$ ($n = 5$, log-rank).

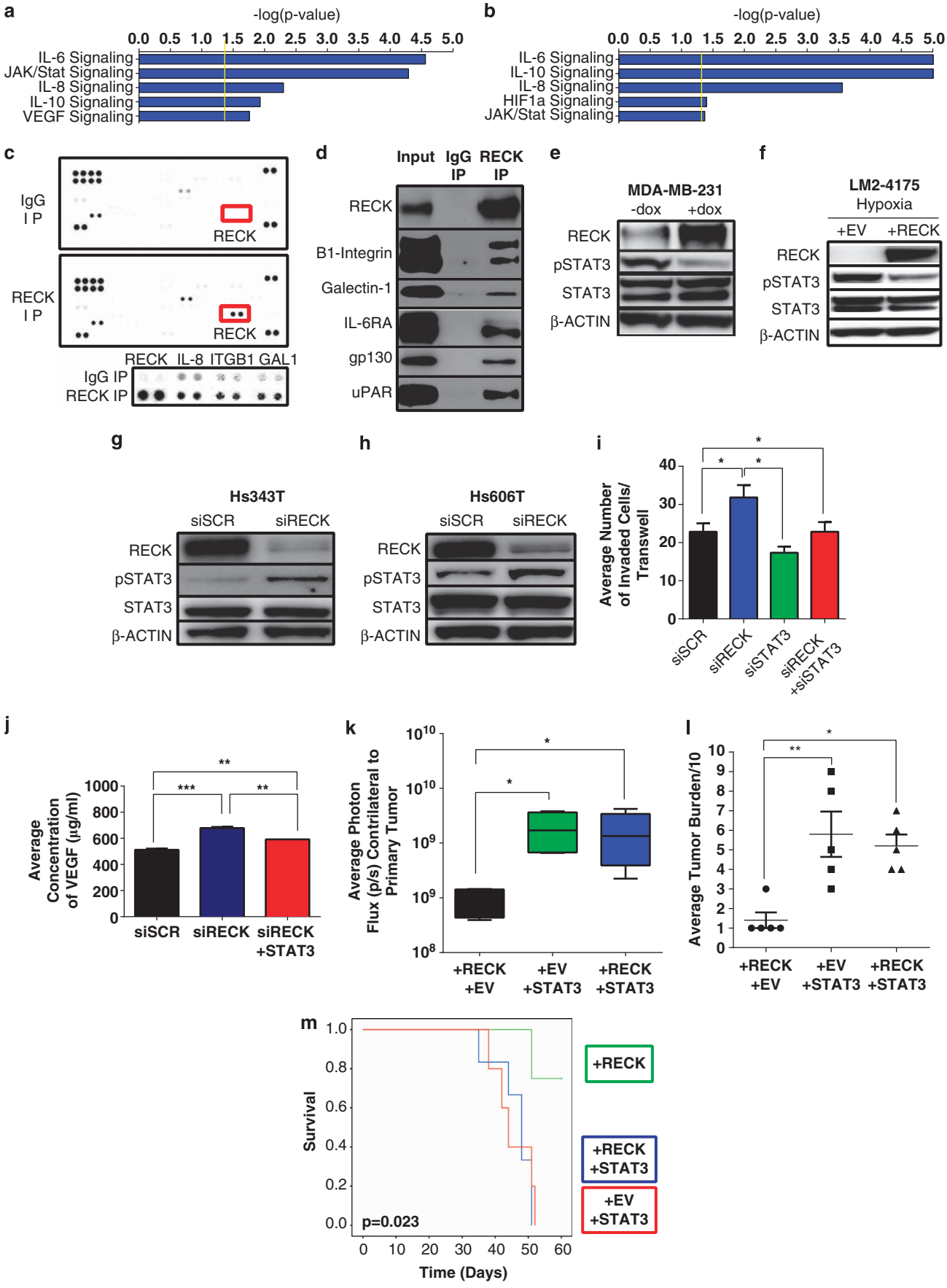

Modulation of metastasis and angiogenesis by RECK is dependent on STAT3 signaling

We next investigated whether the effects of RECK on angiogenesis, invasion and metastasis are STAT3 dependent. First, we determined that the increase in HS606T invasion caused by RECK knockdown was attenuated with the concurrent knockdown of STAT3, demonstrating that RECK-mediated invasiveness is, in part, mediated by STAT3 (Figure 7i, Supplementary Figure S4B). In addition, increased VEGF secretion conferred by RECK knockdown was also attenuated following concurrent knockdown of STAT3 (Figure 7j). This shows that, like the invasion phenotype, RECK-mediated VEGF secretion is also due, at least in part, to STAT3 activation. Finally, we determined whether exogenously expressing STAT3 can reverse the ability of RECK to suppress metastasis. For this, we again made use of our *in vivo* metastasis model. LM2-4175 cells that stably overexpressed RECK were transduced with STAT3 and injected into the mammary fat pad of NSG mice (spontaneous metastasis model). BLI and histological analysis of lung metastasis at day 30 revealed decreased metastasis in mice with cells expressing RECK alone, as expected (Figures 7k and l). This phenotype was attenuated with the concomitant expression of STAT3, suggesting that STAT3 is downstream of RECK and that metastatic suppressive activity of RECK is mediated by STAT3. Using our tail vein *in vivo* metastasis assay and these cells, we found that mice injected with cells expressing RECK has a significant survival advantage that was abrogated by co-expression of STAT3 and RECK ($P = 0.023$, Figure 7m). Together, these results demonstrate that the invasive and angiogenic phenotypes that result from RECK suppression are mediated through STAT3 signaling.

Suppression of RECK expression is associated with poor survival in human breast cancer

Finally, we sought to validate the association of RECK expression with breast cancer survival outcomes and to determine the relationship of RECK loss with pathological covariates. Previous studies linking RECK with clinical outcomes used relatively small numbers of samples. We dichotomized 1586 breast cancer patients from the Curtis data set[30] into 'RECK high' and 'RECK low' groups based on median RECK expression and analyzed disease-specific survival. Here, high RECK expression conferred a significant survival advantage ($P = 0.025$, Figure 8a). This was confirmed in two independent, large breast cancer data sets using identical methodology ($P = 0.006$, Figure 8b,Supplementary Figure S5A). Due to the unique size of the Curtis data set, we were able to further categorize RECK expression as 'normal' or 'low,' based on values in normal breast tissue (Supplementary Figure S5B). Here, 'low' is defined as having an outlier level of RECK expression below the 10th percentile of RECK expression in normal breast tissue. Patients with primary tumors harboring normal RECK expression experienced significantly superior survival compared with those with tumors bearing low RECK ($P = 0.000083$, Figure 8c).

In addition to poorer survival, we found that higher primary tumor grade, cellularity and size were also significantly associated with low RECK expression (Figures 8d–f). RECK expression was not significantly associated with estrogen receptor, progesterone receptor or HER2 status in the Curtis or TCGA breast cancer cohorts (Figures 8g–i, Supplementary Figure S5C–E). Notably, the expression of RECK was significantly decreased in all breast cancer subtypes compared with normal breast tissue (Figures 8j and k, Supplementary Figures S5F and G), suggesting that loss of RECK expression can occur across all breast cancer types. Together these results demonstrate that RECK expression is an important determinant of breast cancer survival, that decreased RECK expression is associated with aggressive tumor characteristics and that RECK alteration is likely selected for in cancers.

DISCUSSION

RECK is recognized as a frequently inactivated metastasis suppressor in a number of human malignancies. Although loss of RECK has been linked to aggressive tumor behavior and metastasis, the molecular mechanisms by which RECK affects these processes is incompletely understood. The effect of RECK on tumor cells has been thought to be attributable to changes in MMP activity. However, in most tumors, these proteases are not predominantly produced by the malignant cells themselves but instead by adjacent stroma.[31] Furthermore, MMP levels in our *in vivo* tumor models do not significantly associate with RECK expression. Accordingly, our data here suggest that, at least in metastatic progression, RECK functions by associating with a number of receptors that signal through STAT3, modulating STAT3 signaling and promoting the coordinated expression of a multifaceted invasion and angiogenic program. As RECK is known to have key roles in normal development,[32,33] we reveal a molecular framework for how RECK regulates metastasis and highlight how metastatic cells can usurp RECK-dependent processes to promote tumor cell survival at distant sites.

We established a significant relationship between RECK expression and disease-specific survival in breast cancer. Through the use of matched pairs of primary human breast tumors and both distant and lymph node metastasis, we show that RECK expression is suppressed in metastatic lesions compared with primary tumors. This is critical as it demonstrates that loss of RECK in metastases is not simply due to sporadic differences between primary tumors but occurs during metastatic progression. Furthermore, as tumor heterogeneity often exists within breast tumors, it would be interesting to determine whether cells with the lowest levels of RECK expression within an individual primary tumor are in fact the founder cells in distant metastases.

Preclinical data and retrospective human studies suggest that MSGs have the potential to improve patient selection for therapy and may predict response to treatment.[34] For example, mechanistic insights into the function of the MSG NM23 have led to the development of novel treatment strategies both exploiting aberrant NM23-associated cell signaling and reconstituting NM23 itself. Clinical trials using NM23 as an anti-metastasis therapy are currently underway.[3] Notably, it has been shown *in vitro* that treating cell lines harboring epigenetically silenced RECK with HDAC or DNA methyltransferase inhibitors can lead to the re-expression of RECK.[35,36] In our study, RECK reconstitution in breast cancer cells significantly decreased metastatic burden in multiple *in vivo* models of metastasis. As such, it may be reasonable to explore new treatment strategies aimed at treating tumors with RECK silencing with epigenetically targeted therapies.

RECK not only affects invasive potential of cancer cells but its loss also supports the survival and expansion of tumor cells in distant organs and tissues. Angiogenesis is a hallmark of cancer, wound healing and various ischemic and inflammatory diseases[37,38] VEGF is a potent inducer of angiogenesis and lymphangiogenesisand is a highly specific mitogen for endothelial cells.[39] Here, we reveal that RECK directly modulates VEGF secretion. Furthermore, RECK convergently regulates multiple pro-and anti-angiogenic factors in a coordinated fashion. These data therefore provide detailed mechanistic insights into the RECK-mediated angiogenic phenotype.[40]

Our data reveal that RECK functions by regulating STAT3 activity. STAT3 activation has been linked to VEGF expression and oncogenesis, but the mechanisms underlying this hyperactivity are not well understood.[41,42] Two primary transcription factors that directly regulate VEGF expression are STAT3 and hypoxia-inducible factor-1α.[43] Induction of VEGF can be achieved by these transcription factors through diverse stimuli, including hypoxia and cytokines. Our data show that RECK binds to many receptors

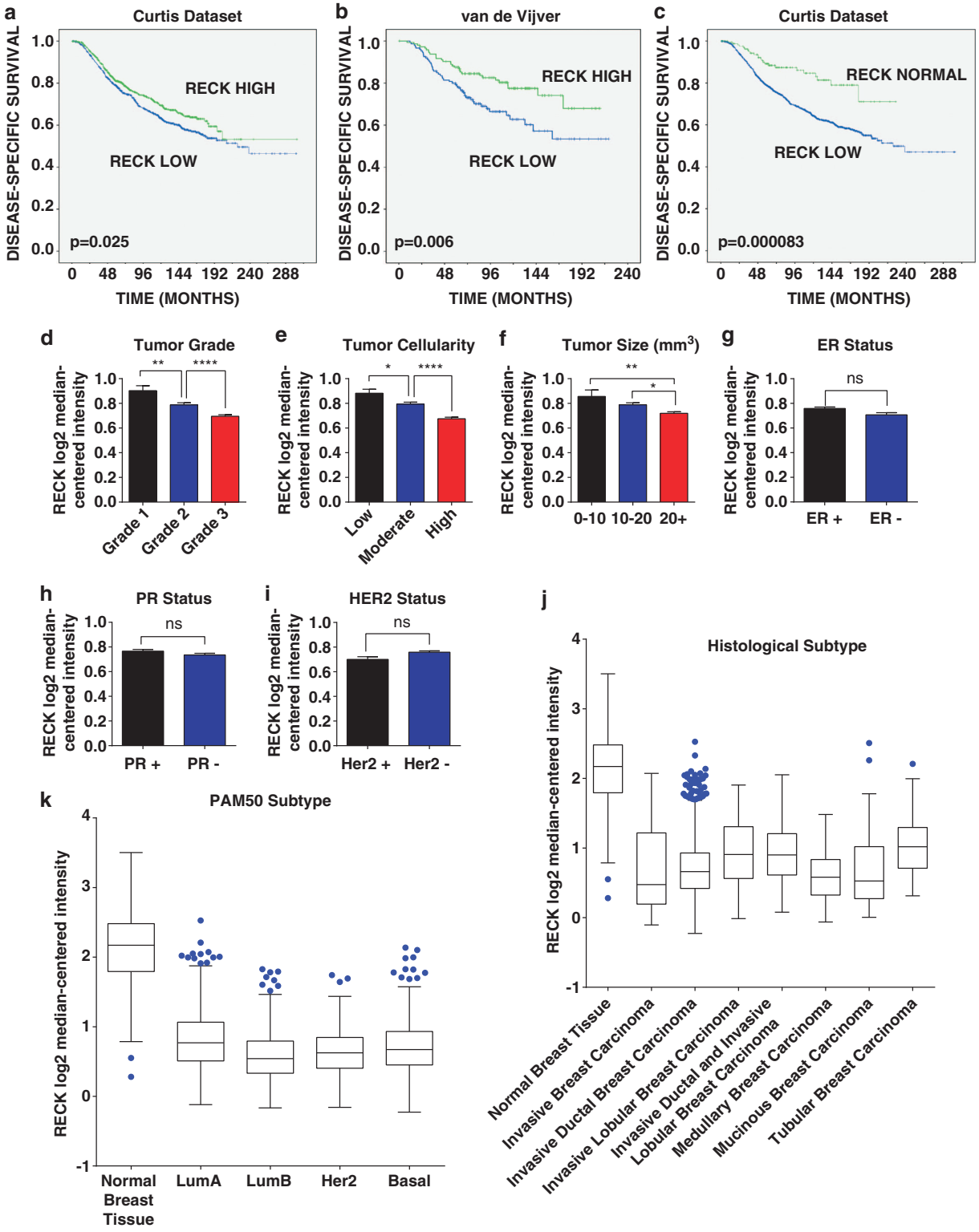

Figure 8. Clinical and pathological correlates of RECK loss in breast cancer. (**a**) Loss of RECK expression is associated with poor clinical outcome. Kaplan–Meier survival plot of 1586 breast cancer patients from the Curtis breast cancer data set separated into 'RECK High' and 'RECK Low' groups based on the median RECK expression ($P = 0.025$, log-rank). (**b**) Kaplan–Meier survival plot of 295 breast cancer patients from the van de Vijver breast cancer data set separated into 'RECK High' and 'RECK Low' groups based on the median RECK expression ($P = 0.006$, log-rank). (**c**) Kaplan–Meier survival plot of 1586 breast cancer patients from the Curtis breast cancer data set separated into 'RECK Normal' and 'RECK Low' groups based on the RECK expression levels in normal breast tissue ($P = 0.000083$, log-rank). See text for rationale. RECK expression from the Curtis breast cancer data set by (**d**) tumor grade in 1902 tumors, (**e**) cellularity in 1927 tumors and (**f**) tumor size in 1972 tumors. RECK expression in tumor sets segregated by (**g**) ER status in 1948 tumors, (**h**) PR status and (**i**) HER2 status in 1992 tumors. All data are presented as mean ± s.e.m. (*$P < 0.05$, **$P < 0.01$, ****$P < 0.0001$, NS = not significant). (**j**) RECK expression based on histological subtype in 2037 breast cancer tumors. Data are presented as Tukey's box plot. (**k**) RECK expression based on PAM50 subtype in 1986 breast cancer tumors. Data are presented as Tukey's box plot.

that are known activators of STAT3 signaling and angiogenesis, including IL-8, galectin-1, B1-integrin, uPAR and the primary activators of STAT3 signaling in breast cancer, IL-6RA and gp130.[23,44–48] Interestingly, it has previously been reported that the inhibition of gp130 signaling in breast cancer blocks STAT3 activation, inhibiting malignancy *in vivo*.[49] It seems that RECK has a central role in coordinating and downregulating the extent of STAT3 activation downstream of these various receptors. This activity, in turn, regulates neovascular programs that are important for metastases. Of note, STAT3 can be activated by phosphorylation at Y705 and/or S727. pSTAT3-Y705, which was assessed in this study, is the STAT3 phosphorylation site that is associated with IL-6 and IL-8 signaling.[50,51] In contrast, STAT3-S727 phosphorylation is associated with cellular proliferation via extracellular signal–regulated kinase signaling and has been shown to inversely correlate with pSTAT3-Y705 levels.[52–55] Here we show that RECK knockdown results in increased pSTAT3-Y705 and decreased pSTAT3-S727 (Supplementary Figures S6A and B). This further supports our model of RECK-mediated STAT3 regulation of metastatic processes via inhibition of IL-mediated STAT3 phosphorylation.

Interestingly, studies focusing on microRNA expression and metastasis have revealed that STAT3 can control microRNAs, which in turn regulates RECK expression.[56] These data combined with the findings in our study point to a feedback loop between RECK, STAT3 and microRNAs. Of note, our study did not see changes in tumorigenecity or primary tumor growth by directly modulating RECK expression. In contrast, studies on microRNAs that modulate RECK do report changes in tumorigenecity, suggesting that RECK expression is just one of the many potential targets of microRNAs.[57]

In our study, we showed that RECK mediated suppression of spontaneous metastasis *in vivo*, which suggests that RECK can affect multiple steps in the metastatic process. Interestingly, RECK suppression was concomitant with increased expression of uPA, a known inducer of breast cancer metastasis. *In vitro*, it has been shown that uPA itself has the capacity to increase the invasiveness of tumor cells,[58] which we have confirmed here using breast cancer cell lines. The uPA system is a serine protease family that includes uPA, uPAR and plasminogen activator inhibitors.[59] uPA catalyzes the activation of plasminogen to plasmin, which degrades the ECM and basement membranes either directly or indirectly through activating pro-MMPs (as most MMPs are secreted as latent zymogens).[60,61] This uPA–RECK relationship may partially explain how most tumors and tumor cell lines secrete very low levels of MMPs, yet retain strong invasive potential. Although MMPs have a clear role in metastasis, *in vivo* studies are complicated owing to the presence of both inactive and active MMPs, whose conversion is catalyzed by other proteases. Further, the cellular origin of secreted MMPs *in vivo* is difficult to ascertain. As a result, we cannot exclude the importance of MMPs in our study, though our discovery of RECK-mediated uPA secretion provides both complimentary (uPA-induced MMP activation) and alternative (direct ECM proteolysis) mechanisms of RECK-associated suppression of metastasis.

In summary, RECK is a multifunctional and broadly important MSG that is frequently suppressed in cancer. Our observations address several ill-defined issues central to the development of metastasis: how a frequently inactivated MSG suppresses metastases, how metastases activate neovascular programs, what signaling mechanisms underlie RECK's control of angiogenesis, and the molecular causes of STAT3 hyperactivity in metastatic lesions. Our work provides critical insights into our understanding of the metastatic process.

MATERIALS AND METHODS

Expression data sets

The van de Vijver[62] and Stockholm[63] breast cancer data sets were downloaded from the Gene Expression Omnibus (GEO http://www.ncbi.nlm.nih.gov/geo). The Curtis data set[30] and the TCGA breast cancer data set[64] were downloaded from http://www.oncomine.org.

Primary human breast cancer and matched lymph node metastases

Paired primary tumor and lymph node metastases were collected during surgical resection. All tissue was used with informed consent and banked at Memorial Sloan-Kettering Cancer Center (MSKCC) in accordance with IRB approval. All samples were snap-frozen and stored at −80 °C until use. All samples were H&E stained and independently reviewed by a breast cancer pathologist. Tumors were microdissected to obtain >70% purity. RNA was isolated from fresh frozen samples using the RNEasy Plus mini prep kit (Qiagen, Valencia, CA, USA). Nucleic acid quality was determined with the Agilent 2100 Bioanalyzer (Agilent Technologies, Santa Clara, CA, USA). Primary tumor and matched metastasis pairs, for which RNA of sufficient quantity and quality was available, were analyzed on Affymetrix GeneChip Human Genome U133 2.0 Array (Affymetrix, Santa Clara, CA, USA) at the genomics core at Sloan-Kettering Institute according to the manufacturer's protocol.

Primary human breast cancer and matched distant metastases

Paired primary tumor and distant metastases were collected with informed consent and banked at MSKCC in accordance with IRB approval. All samples were formalin fixed and paraffin embedded until use. All samples were H&E stained and independently reviewed by a breast cancer pathologist. Samples were also sectioned (5 μm) and immunostained with a RECK antibody and blindly scored.

Microarray analysis of cell lines

Total RNA was isolated from cell lines using the RNEasy Plus mini prep kit (Qiagen). Nucleic acid quality was determined with the Agilent 2100 Bioanalyzer. Samples were analyzed on Affymetrix GeneChip Human Genome U133 2.0 Array at the genomics core at Sloan-Kettering Institute according to the manufacturer's protocol.

Gene expression microarray analysis

Gene expression analysis in cell lines was performed with the Human Genome U133A 2.0 microarray (Affymetrix). CEL files were imported into the Partek Genomics Suite software and normalized using robust multiarray average quartile normalization and log probe summarization. Differentially expressed genes were identified by analysis of variance. Genes that were differentially expressed at $P < 0.05$ and had at least an absolute value of 1.2× fold change (1.5-fold change for Hs343T) were considered significant. Enriched pathways were identified in the differentially expressed genes in Ingenuity pathway analysis (Ingenuity Systems, Valencia, CA, USA) and determined significant at $-\log2(P\text{-value}) > 1.3$ (Supplementary Tables S5–S8).

Animal studies

All animal work was done in accordance with the Institutional Animal Care and Use Committee at MSKCC. Athymic Nu/Nu mice were obtained from Harlan Laboratories (Indianapolis, IN, USA) and NSG mice were obtained from Jackson Laboratories (Bar Harbor, ME, USA). All animals were injected between 5 and 7 weeks of age. Intracardiac injections of BOM1-1833 cells and intravenous injections of LM2-4175 cells were performed as previously described.[13,14] Single-cell suspensions of the indicated cell lines (1×10^6 cells) in 1:1 serum-free media/Matrigel (BD Biosciences, Franklin Lakes, NJ, USA) were injected orthotopically into the mammary fat pad of 6-week-old female NSG mice. Animals were imaged weekly via BLI (IVIS, Xenogen, Alameda, CA, USA).

Cell lines

Hs606T, Hs343T, human umbilical vein endothelial cells (HUVEC), HEK293T and HMEC-hTERT were purchased from the American Type Culture Collection (ATCC, Manassas, VA, USA) and cultured according to ATCC's recommended conditions. MDA-MB-231, LM2-4175 and BOM1-1833 were

all generous gifts from Dr Joan Massague (Memorial Sloan-Kettering Cancer Center, New York, NY, USA) and were cultured as described previously.[13,14]

Cell proliferation assay

In all, 1×10^5 cells were plated in 6-cm plates in triplicate, and cell numbers were counted at the indicated days using a ViCELL cell counter (Beckman, Indianapolis, IN, USA).

Cell cycle analysis

Cells were trypsinized, fixed with ice cold 70% ethanol and stained using 7-AAD. Cell cycle analysis was performed on a FACSCalibur (BD Biosciences). Analysis was performed using the FlowJo software (Flowjo, Ashland, OR, USA), and cell cycle quantification was performed using the Watson (Pragmatic) model.

Immunoblotting

Cell lysates were prepared with CellLytic M (Sigma, St Louis, MO, USA) containing protease and phosphotase inhibitor (Thermo Scientific, Pittsburgh, PA, USA). Debris was removed via centrifugation for 10 min at 14 000 r.p.m. in an Eppendorf Centrifuge 5424C (Eppendorf, Hauppauge, NY, USA) at 4 °C. Protein concentrations were determined by BCA protein assay kit (Thermo Scientific), and equal amounts of protein samples were loaded on NuPAGE Bis-Tris 4–12% sodium dodecyl sulfate gels (Invitrogen, Grand Island, NY, USA) and blotted onto polyvinylidene difluoride membrane (Millipore, Billerica, MA, USA). Imaging was performed on a FujiFilm LAS4000 (GE Healthcare, Pittsburgh, PA, USA) . All blots were repeated three times, and representative images were chosen for publication.

Chemotaxis assay

Conditioned media from the indicated cell types was placed in the bottom chamber of a 12-well plate. HUVEC cells were seeded at a density of 5×10^4/well in transwell inserts placed in the upper chamber (8 μm, BD Biosciences). After incubation for 12 h, migrated cells were quantified by counting on a Nikon TE2000E brightfield microscope, Nikon Instruments, Melville, NY, USA).

ELISA

All ELISA kits were purchased from R&D Systems (Minneapolis, MN, USA) and performed according to manufacturer's instructions. For isolation of conditioned media, equal number of cells was seeded, and media was conditioned overnight. To remove cellular contaminant, conditioned media was collected and centrifuged at 300 *g* for 10 min in an Eppendorf Centrifuge 5424C (Eppendorf) at 4 °C.

Antibody arrays

Proteome Profiler antibody arrays were purchased from R&D Systems and used according to the manufacturer's instructions. Conditioned media was generated as described above (ELISA). Imaging was performed on a FujiFilm LAS4000. Quantification of densitometry was achieved using the ImageQuantTL software (GE Healthcare).

Virus production and generation of stable cell lines

HEK 293T cells were transfected with lentiviral expression constructs using Fugene 6 (Promega) in combination with pCMV-dR8.2 (gag/pol)and VSV-G (env) expression vectors using Fugene 6 (Promega). Viral stocks were collected 48 h posttransfection, filtered (0.45 μm) and placed on target cells for 8 h in the presence of 8 μg/ml polybrene. Forty-eight hours postinfection, cells were selected in the presence of puromycin (2 μg/ml).

RNA interference

Knockdown using scramble and/or gene-specific siRNA (ON-TARGET SMARTpool, Thermo Scientific) was performed using Lipofectamine RNAiMAX (Invitrogen). Stable knockdown was achieved using scramble and RECK-specific shRNA constructs (Thermo Scientific) to generate virus as above (see 'Virus production and generation of stable cell lines').

Chemotaxis assays

HUVEC cells were seeded on 12-well Boyden transwells in serum-free media (8 μm, BD Biosciences). Cells were allowed to migrate towards the indicated conditioned media for 24 h. Cells that did not migrate were removed using a cotton swab. The membranes were then fixed with methanol and stained with DAPI (4,6-diamidino-2-phenylindole). The number of migrated cells was determined by manual counting using an inverted Nikon TE2000E microscope (Nikon Instruments).

Invasion assays

Indicated cells were seeded in serum-free media on Matrigel-coated transwell inserts (8 μm, BD Biosciences). Complete media was placed below transwell inserts to encourage cell invasion. After 24 h, cells that did not invade were removed using a cotton swab. Membranes were then fixed with methanol and stained with DAPI. The number of invaded cells was determined by manual counting using an inverted Nikon fluorescent microscope.

IHC and analysis

The IHC detection of indicated antibodies was performed at Molecular Cytology Core Facility of MSKCC using Discovery XT processor (Ventana Medical Systems, Tucson, AR, USA). The tissue sections were deparaffinized with EZPrep buffer (Ventana Medical Systems), antigen retrieval was performed with CC1 buffer (Ventana Medical Systems) and sections were blocked for 30 min with Background Buster solution (Innovex, Richmond, CA, USA) (for rabbit, mouse and chicken antibodies, for rat and goat antibodies it should be 10% normal rabbit serum in phosphate-buffered saline+2% BSA (bovine serum albumin)). Antibodies were applied, and sections were incubated for 5 h, followed by 60 min incubation with biotinylated goat anti-rabbit IgG (Vector Laboratories, Burlingame, CA, USA, cat. no. PK6101) (biotinylated horse anti-mouse IgG (Vector Laboratories, cat. no. MKB-22258); biotinylated goat anti-chicken (Vector Laboratories, cat. no. BA-9010); biotinylated rabbit anti-goat IgG (Vector Laboratories, cat. no. BA-5000)) at 1:200 dilution. The detection was performed with DAB detection kit (Ventana Medical Systems) according to the manufacturer's instruction. Slides were counterstained with hematoxylin and coverslipped with Permount (Fisher Scientific, Waltham, MA USA). Staining quantification was performed using the MetaMorph software (MetaMorph, Nashville, TN, USA).

Immunofluorescence

Cells were grown as monolayer cultures on D-polylysine-coated coverslips and were fixed with 4% paraformaldehyde. After washing three times with phosphate-buffered saline, cells were blocked for 30 min with 10% goat serum and incubated overnight at 4 °C with primary antibodies against RECK (1:50, R&D Systems). Cells were then stained with Alexa Fluor 563 secondary antibody (1:200, Invitrogen) for 1 h at room temperature. Stained sections and cells were mounted in ProLong Gold antifade reagent (Invitrogen) with DAPI. Images were taken on a Leica TCS SP5 confocal microscope (Leica Microsystems, Buffalo Grove, IL, USA).

Quantitative real-time PCR

Total RNA was isolated from cells using RNEasy Plus according to the manufacturer's instructions (Qiagen). cDNA was generated using 1 μg RNA and cDNA EcoDry Premix (Clontech, Mountain View, CA, USA). qRT–PCR was performed using a Realplex2 Mastercycler (Eppendorf) and analyzed by standard delta relative quantitation (ΔΔRQ). qRT–PCR parameters were as follows: initial denaturation at 95 °C for 5 min, then 40 cycles of 95 °C 15 s and 60 °C 1 min. Primers used: RECK—Forward 5′-TGCAAGCAGGC ATCTTCAAA-3′ Reverse 5′-ACCGAGCCCATTTCATTTCTG-3′; and GAPDH—Forward 5′-AATGAAGGGGTCATTGATGG-3′ Reverse5′-AAGGTGAAGGTCG GAGTCAA-3′.

Endothelial tube formation assay

Endothelial cells (HUVEC) were resuspended in the indicated conditioned media and grown for 6 h on Matrigel (BD biosciences). Tube formation was quantified by calculating the average number of branch points in 10 fields of view. Imaging was performed using a Nikon TE2000-E inverted microscope. Representative images were chosen for publication from three replicates.

Immunoprecipitation

For immunoprecipitation, 50 µl of protein G magnetic beads (PureProteome, Millipore) were crosslinked with 10 µg anti-RECK goat polyclonal antibody (R&D Systems) or goat polyclonal IgG antibody (R&D Systems) using 5 mM BS^3 according to the manufacturer's instructions (protocol guide, Millipore). Confluent Hs606T whole-cell lysates (500 µg total protein) were incubated with crosslinked beads at 4 °C overnight with gentle agitation. The immunocomplexes were washed three times with TBS-T (0.1%), bound protein eluted in 60 µl 0.2 M glycine-HCl (pH 2.5) and neutralized using 5 µl of 1 M Tris (pH 8.5). Eluates were then used to probe an antibody array (Human Soluble Receptor Antibody Array, Non-Hematopoietic Panel, R&D Systems). This array was modified by using immunoprecipitated eluate instead of conditioned media or cell lysate. Eluates were also subjected to sodium dodecyl sulfate-polyacrylamide gel electrophoresis and western blotting analysis for RECK (goat antibody, R&D Systems), uPAR (goat antibody, R&D Systems), galectin-1 (rabbit antibody, Cell Signaling, Beverly, MA, USA), and integrin β1 (rabbit antibody, Cell Signaling).

Statistical analysis

For survival analysis, survival curves were analyzed using the Kaplan–Meier method and log rank test with the IBM Statistica 20 software (IBM, Road Armonk, NY, USA). All other statistical analysis was performed using the Prism 6 Software (GraphPad Software, La Jolla, CA, USA).

Kinexus antibody microarray

Protein lysates were sent to Kinexus Bioinformatics Corporation (Vancouver, BC, Canada) and profiled using their Kinex 850 Antibody Microarray (KAM). All samples were normalized according to the Kinexus normalization guidelines, and a list of downregulated candidate proteins was generated.

Antibodies

Antibody	*Supplier*	*Cat. no.*
Actin	Sigma	A3853
CD34	abCAM	ab8158
Galectin-1	Cell Signaling	5418S
Ki67	abCAM	ab16667
MMP-2	R&D	AF902
MMP-9	R&D	AF911
MT1-MMP	R&D	AF918
pSTAT3 (Tyr705)	Cell Signaling	9145S
pSTAT3 (Ser727)	Cell Signaling	9136
RECK	R&D	AF1734
STAT3	Cell Signaling	9139S
uPA	R&D	AF1310
uPAR	R&D	AF807
VEGF	Santa Cruz	sc-507
β1-Integrin	Cell Signaling	4706P

Microarray accession numbers

Gene Expression Omnibus (GEO)—accession number GSE56898.

CONFLICT OF INTEREST

The authors declare no conflict of interest.

ACKNOWLEDGEMENTS

We thank Agnes Viale and Russell Towers for technical assistance. We are indebted to Joan Massague (Memorial Sloan-Kettering Cancer Center) for generously providing cell lines and some constructs. We are grateful to the entire Tumour Procurement Service at MSKCC for facilitating tissue procurement and contributing valuable input. This work was supported by grants from the Department of Defense (DOD) (grant no. BC120568), the Frederick Adler Fund, the Avon Foundation, the Elsa Pardee foundation, the MSKCC Metastasis Center and the STARR Cancer Consortium (all to TAC). LAW was supported by The Canadian Institutes of Health Research PDF Award MFE-127325. DMR was supported by the HHMI Research Fellows Program and NIH MSTP grant T32GM007739. AS was supported by the Ruth L. Kirschstein National Research Award (NRSA) number T32CA009512 from the National Cancer Institute. ST was supported by an NIH T32 grant (5T32CA160001).

AUTHOR CONTRIBUTIONS

LAW and DMR designed, performed and analyzed the experiments and aided in writing the manuscript. MR, DG, AS, ST, CAB, JL, JB and TAK contributed to the completion of various experiments. LAW and TAC conceived the study, supervised the research and contributed to writing the manuscript.

REFERENCES

1 Gonzalez-Angulo AM, Morales-Vasquez F, Hortobagyi GN. Overview of resistance to systemic therapy in patients with breast cancer. *Adv Exp Med Biol* 2007; **608**: 1–22.
2 Cardoso F, Harbeck N, Fallowfield L, Kyriakides S, Senkus E, Group EGW. Locally recurrent or metastatic breast cancer: ESMO Clinical Practice Guidelines for diagnosis, treatment and follow-up. *Ann Oncol* 2012; **23** (Suppl 7): vii11–vii19.
3 Shoushtari AN, Szmulewitz RZ, Rinker-Schaeffer CW. Metastasis-suppressor genes in clinical practice: lost in translation? *Nat Rev Clin Oncol* 2011; **8**: 333–342.
4 Noda M, Takahashi C, Matsuzaki T, Kitayama H. What we learn from transformation suppressor genes: lessons from RECK. *Future Oncol* 2010; **6**: 1105–1116.
5 Rabien A, Ergun B, Erbersdobler A, Jung K, Stephan C. RECK overexpression decreases invasive potential in prostate cancer cells. *Prostate* 2012; **72**: 948–954.
6 Chang CK, Hung WC, Chang HC. The Kazal motifs of RECK protein inhibit MMP-9 secretion and activity and reduce metastasis of lung cancer cells in vitro and in vivo. *J Cell Mol Med* 2008; **12**(6B): 2781–2789.
7 Oh J, Takahashi R, Kondo S, Mizoguchi A, Adachi E, Sasahara RM *et al.* The membrane-anchored MMP inhibitor RECK is a key regulator of extracellular matrix integrity and angiogenesis. *Cell* 2001; **107**: 789–800.
8 Zhang C, Ling Y, Zhang C, Xu Y, Gao L, Li R *et al.* The silencing of RECK gene is associated with promoter hypermethylation and poor survival in hepatocellular carcinoma. *Int J Biol Sci* 2012; **8**: 451–458.
9 Chang HC, Cho CY, Hung WC. Silencing of the metastasis suppressor RECK by RAS oncogene is mediated by DNA methyltransferase 3b-induced promoter methylation. *Cancer Res* 2006; **66**: 8413–8420.
10 Hill VK, Ricketts C, Bieche I, Vacher S, Gentle D, Lewis C *et al.* Genome-wide DNA methylation profiling of CpG islands in breast cancer identifies novel genes associated with tumorigenicity. *Cancer Res* 2011; **71**: 2988–2999.
11 Ishikawa S, Takenaka K, Yanagihara K, Miyahara R, Kawano Y, Otake Y *et al.* Matrix metalloproteinase-2 status in stromal fibroblasts, not in tumor cells, is a significant prognostic factor in non-small-cell lung cancer. *Clin Cancer Res* 2004; **10**: 6579–6585.
12 Roomi MW, Monterrey JC, Kalinovsky T, Rath M, Niedzwiecki A. Patterns of MMP-2 and MMP-9 expression in human cancer cell lines. *Oncol Rep* 2009; **21**: 1323–1333.
13 Kang Y, Siegel PM, Shu W, Drobnjak M, Kakonen SM, Cordon-Cardo C *et al.* A multigenic program mediating breast cancer metastasis to bone. *Cancer Cell* 2003; **3**: 537–549.
14 Minn AJ, Gupta GP, Siegel PM, Bos PD, Shu W, Giri DD *et al.* Genes that mediate breast cancer metastasis to lung. *Nature* 2005; **436**: 518–524.
15 Zhang B, Zhang J, Xu ZY, Xie HL. Expression of RECK and matrix metalloproteinase-2 in ameloblastoma. *BMC Cancer* 2009; **9**: 427.
16 Cardeal LB, Boccardo E, Termini L, Rabachini T, Andreoli MA, di Loreto C *et al.* HPV16 oncoproteins induce MMPs/RECK-TIMP-2 imbalance in primary keratinocytes: possible implications in cervical carcinogenesis. *PLoS One* 2012; **7**: e33585.
17 Dong Q, Yu D, Yang CM, Jiang B, Zhang H. Expression of the reversion-inducing cysteine-rich protein with Kazal motifs and matrix metalloproteinase-14 in neuroblastoma and the role in tumour metastasis. *Int J Exp Pathol* 2010; **91**: 368–373.
18 Zarogoulidis P, Yarmus L, Darwiche K, Walter R, Huang H, Li Z *et al.* Interleukin-6 cytokine: a multifunctional glycoprotein for cancer. *Immunome Res* 2013; **9**: 16535.
19 Rosenkilde MM, Schwartz TW. The chemokine system -- a major regulator of angiogenesis in health and disease. *APMIS* 2004; **112**: 481–495.
20 Zeng L, O'Connor C, Zhang J, Kaplan AM, Cohen DA. IL-10 promotes resistance to apoptosis and metastatic potential in lung tumor cell lines. *Cytokine* 2010; **49**: 294–302.
21 Tang L, Han X. The urokinase plasminogen activator system in breast cancer invasion and metastasis. *Biomed Pharmacother* 2013; **67**: 179–182.
22 Chaffer CL, Weinberg RA. A perspective on cancer cell metastasis. *Science* 2011; **331**: 1559–1564.
23 Berishaj M, Gao SP, Ahmed S, Leslie K, Al-Ahmadie H, Gerald WL *et al.* Stat3 is tyrosine-phosphorylated through the interleukin-6/glycoprotein 130/Janus kinase pathway in breast cancer. *Breast Cancer Res* 2007; **9**: R32.
24 Bournazou E, Bromberg J. Targeting the tumor microenvironment: JAK-STAT3 signaling. *JAKSTAT* 2013; **2**: e23828.

25 Huang C, Xie K. Crosstalk of Sp1 and Stat3 signaling in pancreatic cancer pathogenesis. *Cytokine Growth Factor Rev* 2012; **23**(1-2): 25–35.
26 Kim JH, Lee SC, Ro J, Kang HS, Kim HS, Yoon S. Jnk signaling pathway-mediated regulation of Stat3 activation is linked to the development of doxorubicin resistance in cancer cell lines. *Biochem Pharmacol* 2010; **79**: 373–380.
27 Benasciutti E, Pages G, Kenzior O, Folk W, Blasi F, Crippa MP. MAPK and JNK transduction pathways can phosphorylate Sp1 to activate the uPA minimal promoter element and endogenous gene transcription. *Blood* 2004; **104**: 256–262.
28 Jung JE, Lee HG, Cho IH, Chung DH, Yoon SH, Yang YM *et al.* STAT3 is a potential modulator of HIF-1-mediated VEGF expression in human renal carcinoma cells. *FASEB J* 2005; **19**: 1296–1298.
29 Kang SH, Yu MO, Park KJ, Chi SG, Park DH, Chung YG. Activated STAT3 regulates hypoxia-induced angiogenesis and cell migration in human glioblastoma. *Neurosurgery* 2010; **67**: 1386–1395, discussion 95.
30 Curtis C, Shah SP, Chin SF, Turashvili G, Rueda OM, Dunning MJ *et al.* The genomic and transcriptomic architecture of 2000 breast tumours reveals novel subgroups. *Nature* 2012; **486**: 346–352.
31 Zucker S, Cao J, Chen WT. Critical appraisal of the use of matrix metalloproteinase inhibitors in cancer treatment. *Oncogene* 2000; **19**: 6642–6650.
32 Prendergast A, Linbo TH, Swarts T, Ungos JM, McGraw HF, Krispin S *et al.* The metalloproteinase inhibitor Reck is essential for zebrafish DRG development. *Development* 2012; **139**: 1141–1152.
33 Chandana EP, Maeda Y, Ueda A, Kiyonari H, Oshima N, Yamamoto M *et al.* Involvement of the Reck tumor suppressor protein in maternal and embryonic vascular remodeling in mice. *BMC Dev Biol* 2010; **10**: 84.
34 Prabhu VV, Siddikuzzaman, Grace VM, Guruvayoorappan C. Targeting tumor metastasis by regulating Nm23 gene expression. *Asian Pac J Cancer Prev* 2012; **13**: 3539–3548.
35 Jeon HW, Lee YM. Inhibition of histone deacetylase attenuates hypoxia-induced migration and invasion of cancer cells via the restoration of RECK expression. *Mol Cancer Ther* 2010; **9**: 1361–1370.
36 Cho CY, Wang JH, Chang HC, Chang CK, Hung WC. Epigenetic inactivation of the metastasis suppressor RECK enhances invasion of human colon cancer cells. *J Cell Physiol* 2007; **213**: 65–69.
37 Hoeben A, Landuyt B, Highley MS, Wildiers H, Van Oosterom AT, De Bruijn EA. Vascular endothelial growth factor and angiogenesis. *Pharmacol Rev* 2004; **56**: 549–580.
38 Hanahan D, Weinberg RA. Hallmarks of cancer: the next generation. *Cell* 2011; **144**: 646–674.
39 Byrne AM, Bouchier-Hayes DJ, Harmey JH. Angiogenic and cell survival functions of vascular endothelial growth factor (VEGF). *J Cell Mol Med* 2005; **9**: 777–794.
40 Sasahara RM, Brochado SM, Takahashi C, Oh J, Maria-Engler SS, Granjeiro JM *et al.* Transcriptional control of the RECK metastasis/angiogenesis suppressor gene. *Cancer Detect Prev* 2002; **26**: 435–443.
41 Carbajo-Pescador S, Ordonez R, Benet M, Jover R, Garcia-Palomo A, Mauriz JL *et al.* Inhibition of VEGF expression through blockade of Hif1alpha and STAT3 signalling mediates the anti-angiogenic effect of melatonin in HepG2 liver cancer cells. *Br J Cancer* 2013; **109**: 83–91.
42 Bid HK, Oswald D, Li C, London CA, Lin J, Houghton PJ. Anti-angiogenic activity of a small molecule STAT3 inhibitor LLL12. *PLoS One* 2012; **7**: e35513.
43 Xu Q, Briggs J, Park S, Niu G, Kortylewski M, Zhang S *et al.* Targeting Stat3 blocks both HIF-1 and VEGF expression induced by multiple oncogenic growth signaling pathways. *Oncogene* 2005; **24**: 5552–5560.
44 Avraamides CJ, Garmy-Susini B, Varner JA. Integrins in angiogenesis and lymphangiogenesis. *Nature Rev Cancer* 2008; **8**: 604–617.
45 Shain KH, Yarde DN, Meads MB, Huang M, Jove R, Hazlehurst LA *et al.* Beta1 integrin adhesion enhances IL-6-mediated STAT3 signaling in myeloma cells: implications for microenvironment influence on tumor survival and proliferation. *Cancer Res* 2009; **69**: 1009–1015.
46 D'Haene N, Sauvage S, Maris C, Adanja I, Le Mercier M, Decaestecker C *et al.* VEGFR1 and VEGFR2 involvement in extracellular galectin-1- and galectin-3-induced angiogenesis. *PLoS One* 2013; **8**: e67029.
47 Le QT, Shi G, Cao H, Nelson DW, Wang Y, Chen EY *et al.* Galectin-1: a link between tumor hypoxia and tumor immune privilege. *J Clin Oncol* 2005; **23**: 8932–8941.
48 Waugh DJ, Wilson C. The interleukin-8 pathway in cancer. *Clin Cancer Res* 2008; **14**: 6735–6741.
49 Selander KS, Li L, Watson L, Merrell M, Dahmen H, Heinrich PC *et al.* Inhibition of gp130 signaling in breast cancer blocks constitutive activation of Stat3 and inhibits in vivo malignancy. *Cancer Res* 2004; **64**: 6924–6933.
50 Sriuranpong V, Park JI, Amornphimoltham P, Patel V, Nelkin BD, Gutkind JS. Epidermal growth factor receptor-independent constitutive activation of STAT3 in head and neck squamous cell carcinoma is mediated by the autocrine/paracrine stimulation of the interleukin 6/gp130 cytokine system. *Cancer Res* 2003; **63**: 2948–2956.
51 Lee MM, Chui RK, Tam IY, Lau AH, Wong YH. CCR1-mediated STAT3 tyrosine phosphorylation and CXCL8 expression in THP-1 macrophage-like cells involve pertussis toxin-insensitive Galpha(14/16) signaling and IL-6 release. *J Immunol* 2012; **189**: 5266–5276.
52 Chung J, Uchida E, Grammer TC, Blenis J. STAT3 serine phosphorylation by ERK-dependent and -independent pathways negatively modulates its tyrosine phosphorylation. *Mol Cell Biol* 1997; **17**: 6508–6516.
53 Onishi A, Chen Q, Humtsoe JO, Kramer RH. STAT3 signaling is induced by intercellular adhesion in squamous cell carcinoma cells. *Exp Cell Res* 2008; **314**: 377–386.
54 Gu FM, Li QL, Gao Q, Jiang JH, Huang XY, Pan JF *et al.* Sorafenib inhibits growth and metastasis of hepatocellular carcinoma by blocking STAT3. *World J Gastroenterol* 2011; **17**: 3922–3932.
55 Huang G, Yan H, Ye S, Tong C, Ying QL. STAT3 phosphorylation at tyrosine 705 and serine 727 differentially regulates mouse ES cell fates. *Stem Cells* 2013; **32**: 1149–1160.
56 Lin HY, Chiang CH, Hung WC. STAT3 upregulates miR-92a to inhibit RECK expression and to promote invasiveness of lung cancer cells. *Br J Cancer* 2013; **109**: 731–738.
57 Han L, Yue X, Zhou X, Lan FM, You G, Zhang W *et al.* MicroRNA-21 expression is regulated by beta-catenin/STAT3 pathway and promotes glioma cell invasion by direct targeting RECK. *CNS Neurosci Ther* 2012; **18**: 573–583.
58 Thummarati P, Wijitburaphat S, Prasopthum A, Menakongka A, Sripa B, Tohtong R *et al.* High level of urokinase plasminogen activator contributes to cholangiocarcinoma invasion and metastasis. *World J Gastroenterol* 2012; **18**: 244–250.
59 Duffy MJ. The urokinase plasminogen activator system: role in malignancy. *Curr Pharmaceut Des* 2004; **10**: 39–49.
60 Zhao Y, Lyons CE Jr., Xiao A, Templeton DJ, Sang QA, Brew K *et al.* Urokinase directly activates matrix metalloproteinases-9: a potential role in glioblastoma invasion. *Biochem Biophys Res Commun* 2008; **369**: 1215–1220.
61 Choong PF, Nadesapillai AP. Urokinase plasminogen activator system: a multifunctional role in tumor progression and metastasis. *Clin Orthop Relat Res* 2003; **415**(Suppl): S46–S58.
62 van de Vijver MJ, He YD, van't Veer LJ, Dai H, Hart AA, Voskuil DW *et al.* A gene-expression signature as a predictor of survival in breast cancer. *N Engl J Med* 2002; **347**: 1999–2009.
63 Pawitan Y, Bjohle J, Amler L, Borg AL, Egyhazi S, Hall P *et al.* Gene expression profiling spares early breast cancer patients from adjuvant therapy: derived and validated in two population-based cohorts. *Breast Cancer Res* 2005; **7**: R953–R964.
64 Cancer Genome Atlas Network, Comprehensive molecular portraits of human breast tumours. *Nature* 2012; **490**: 61–70.

Supplementary Information accompanies this paper on the Oncogene website (http://www.nature.com/onc)